

Density profiles in a quantum Coulomb fluid near a hard wall

J.-N. Aqua* and F. Cornu†

March 22, 2022

Abstract

Equilibrium particle densities near a hard wall are studied for a quantum fluid made of point charges which interact via Coulomb potential without any regularization. In the framework of the grand-canonical ensemble, we use an equivalence with a classical system of loops with random shapes, based on the Feynman-Kac path-integral representation of the quantum Gibbs factor. After systematic resummations of Coulomb divergences in the Mayer fugacity expansions of loop densities, there appears a screened potential ϕ . It obeys an inhomogeneous Debye-Hückel equation with an effective screening length which depends on the distance from the wall. The formal solution for ϕ can be expanded in powers of the ratios of the de Broglie thermal wavelengths λ_α 's of each species α and the limit of the screening length far away from the wall. In a regime of low degeneracy and weak coupling, exact analytical density profiles are calculated at first order in two independent parameters. Because of the vanishing of wave-functions close to the wall, density profiles vanish gaussianly fast in the vicinity of the wall over distances λ_α 's, with an essential singularity in Planck constant \hbar . When species have different masses, this effect is equivalent to the appearance of a quantum surface charge localized on the wall and proportional to \hbar at leading order. Then, density profiles, as well as the electrostatic potential drop created by the charge-density profile, also involve a term linear in \hbar and which decays exponentially fast over the classical Debye screening length ξ_D . The corresponding contribution to

*Laboratoire de Physique (Laboratoire associé au Centre National de la Recherche Scientifique – UMR 5672), École Normale Supérieure de Lyon, 46 allée d'Italie, 69364 Lyon FRANCE. Present address : Institute for Physical Science and Technology, University of Maryland, College Park, Maryland 20910, USA.

†Laboratoire de Physique Théorique (Laboratoire associé au Centre National de la Recherche Scientifique - UMR 8627), Université Paris-Sud, Bâtiment 210, 91405 Orsay, FRANCE.

the global surface charge exactly compensates the charge in the very vicinity of the surface, so that the net electric field vanishes in the bulk, as it should.

KEYWORDS : Coulomb interactions, quantum mechanics, hard wall, grand-canonical ensemble, inhomogeneous Debye equation, surface charge.

1 Introduction

1.1 Issue at stake

In the present paper the equilibrium density profiles in a quantum fluid of point charges are studied in the vicinity of an impenetrable hard wall. The wall, which occupies the semi-infinite region $x < 0$, has no internal structure and its dielectric constant is the same as that of the medium where charges move. On the contrary, the fluid made of n_s particle species is described at the microscopic level in the framework of quantum statistical mechanics. Two point charges e_α and $e_{\alpha'}$ (where α is a species index) interact via the electrostatic interaction $e_\alpha e_{\alpha'} v(\mathbf{r} - \mathbf{r}')$, where

$$v(\mathbf{r} - \mathbf{r}') = \frac{1}{|\mathbf{r} - \mathbf{r}'|} \quad (1.1)$$

in Gauss units. (The charge e_α includes a factor $1/\sqrt{\epsilon_m}$ in energy terms when charges are embedded in a continuous medium with a relative dielectric constant ϵ_m with respect to the vacuum.) The interaction is translationally invariant, and the anisotropy lies only in the geometric constraint enforced by the presence of the wall. The exact analytical expressions of the density profiles $\rho_\alpha(x)$'s are obtained in a regime where exchange effects are negligible and where Coulomb coupling is weak. Results hold for the electron-hole gas in an intrinsic semi-conductor in the vicinity of a junction or for a dilute and hot quantum plasma near a vessel wall.

The interesting point of the model is that it exhibits how a quantum charge effect, gaussianly localized over de Broglie thermal wavelengths in the vicinity of the wall, is carried by long-range Coulomb interactions up to larger distances from the wall, with an exponential decay over a scale equal to the coulombic screening length. Indeed, whereas the density in a classical ideal gas is uniform in the whole region $x > 0$ and is discontinuous on the wall surface, the quantum density is continuous and vanishes at $x = 0$, because of the continuity of wave-functions and their cancellation inside the impenetrable wall. At the inverse temperature $\beta = 1/k_B T$ (where k_B is Boltzmann constant), in a low-degeneracy limit quantum statistics is reduced to Maxwell-Boltzmann statistics, and the density $\rho_\alpha^{\text{id}}(x)$ of species

α in an ideal gas with quantum dynamics vanishes gaussianly fast over the scale of the thermal de Broglie wavelength λ_α ,

$$\rho_\alpha^{\text{id}}(x) = \rho_\alpha^B \left(1 - e^{-2x^2/\lambda_\alpha^2}\right) + \rho_\alpha^B \mathcal{O}\left(\left(\frac{\lambda_\alpha}{a_\alpha}\right)^3\right). \quad (1.2)$$

In (1.2) ρ_α^B is the bulk density for species α , and

$$\lambda_\alpha = \hbar \sqrt{\frac{\beta}{m_\alpha}}, \quad (1.3)$$

where \hbar is Planck constant and m_α is the mass of species α . The quantum expression with Maxwell-Boltzmann statistics (1.2) is valid up to terms of order $(\lambda_\alpha/a_\alpha)^3$, where a_α is the mean interparticle distance between particles of the same species α ($(4/3)\pi\rho_\alpha^B a_\alpha^3 = 1$).

When Coulomb interactions are taken into account, there arises only one third typical length scale, because Coulomb interactions are scale-invariant. Then only two independent dimensionless parameters rule the physical regimes of the system: the degeneracy parameter and the Coulomb coupling parameter. The degeneracy parameter is $(\lambda/a)^3$, where $\lambda = \sup_\alpha \{\lambda_\alpha\}$ and a is a typical mean interparticle distance. When exchange effects are negligible,

$$\left(\frac{\lambda}{a}\right)^3 \ll 1. \quad (1.4)$$

The third length scale may be chosen to be either the classical screening length ξ_D

$$\xi_D^{-1} = \kappa_D \equiv \sqrt{4\pi\beta \sum_{\alpha=1}^{n_s} \rho_\alpha^B e_\alpha^2} \quad (1.5)$$

or the Landau length βe^2 , namely the classical closest approach distance between two typical like-charges e with kinetic energy of order $1/\beta$. Henceforth, the classical Coulomb coupling parameter can be chosen to be equal either to the ratios $(a/\xi_D)^3$, $\beta e^2/a \equiv \Gamma$, or $\beta e^2/\xi_D \equiv 2\varepsilon_D$. These ratios are proportional to one another,

$$\left(\frac{a}{\xi_D}\right)^3 \propto \varepsilon_D \propto \Gamma^{3/2}. \quad (1.6)$$

More precisely they are linked by the relations $(a/\xi_D)^3 = C\varepsilon_D$ and $\varepsilon_D = [C/8]^{1/2} \Gamma^{3/2}$, where C is a numerical factor which depends on the composition of the fluid through ξ_D and on the relation between a and bulk densities. In a weak-coupling regime

$$\left(\frac{a}{\xi_D}\right)^3 \ll 1. \quad (1.7)$$

When both (1.4) and (1.7) are satisfied,

$$\lambda \ll a \ll \xi_D. \quad (1.8)$$

Therefore, the low-degeneracy and weak-coupling regime is also a regime where $\kappa_D \lambda \ll 1$.

1.2 Results

In the low-degeneracy and weak-coupling regime defined by (1.4) and (1.7), the analytical expression for the profile density $\rho_\alpha(x)$ is calculated in a subregime where the first coupling correction, of order $\varepsilon_D = \kappa_D \beta e^2/2$, and the first diffraction correction, of order $\kappa_D \lambda$, dominate other coupling and exchange corrections. At order ε_D classical contributions do not involve the short-range cut-off that must be introduced in order to prevent the collapse of the system in the limit where \hbar tends to zero. As shown in Section 5, the subregime corresponds to a scaling where

$$\varepsilon_D^2 \leq \left(\frac{\lambda}{a}\right)^3 \ll \varepsilon_D. \quad (1.9)$$

(1.9) can be reexpressed as $\varepsilon_D^3 \leq (\kappa_D \lambda)^3 \ll \varepsilon_D^2$, since $(\lambda/a) \propto \kappa_D \lambda / \varepsilon_D^{1/3}$ by virtue of (1.6). In the subregime (1.9) the density profile in the region $x > 0$ reads

$$\begin{aligned} \rho_\alpha(x) = & \rho_\alpha^B \left(1 - e^{-2x^2/\lambda_\alpha^2}\right) \\ & \times \left[1 - \frac{1}{2} \kappa_D \beta e_\alpha^2 \overline{L}(\kappa_D x) - \beta e_\alpha \Phi(x)\right] + \rho_\alpha^B o(\varepsilon_D, \kappa_D \lambda) \end{aligned} \quad (1.10)$$

where $o(\varepsilon_D, \kappa_D \lambda)$ denotes a sum of terms which tend to zero faster than either ε_D or $\kappa_D \lambda$ when these parameters vanish (See (5.2)). When the latter terms are neglected, $\rho_\alpha(x)$ appears as the product of the ideal-gas density (1.2) with a function arising from interaction corrections. (The generic properties of density profiles are discussed in Section 6.)

The density profile (1.10) results from the combination of three effects: first, the vanishing of quantum wave-functions in the vicinity of the wall; second, the geometric repulsion from the wall [1], described by the classical part of the screened self-energy due to the deformation of screening clouds, $(1/2)\kappa_D \beta e_\alpha^2 \overline{L}(u)$, given in (5.14); third, the interaction $e_\alpha \Phi(x)$ with the electrostatic potential drop $\Phi(x)$ with respect to the bulk, which is created by the charge density profile $\sum_\gamma e_\gamma \rho_\gamma(x)$ itself. (The sign of the latter interaction depends on the sign of e_α .) The potential drop $\Phi(x)$ in (1.10) is the sum of a classical contribution [1] and a quantum “diffraction” effect, linear in \hbar ,

$$\Phi(x) = \Phi^{\text{cl}(\varepsilon_D)}(x) + \Phi^{\text{qu}(\kappa_D \lambda)}(x). \quad (1.11)$$

$\Phi^{\text{cl}(\varepsilon_D)}(x)$, of order $\varepsilon_D/(\beta e)$, is written in (5.40) and $\Phi^{\text{qu}(\kappa_D \lambda)}(x)$, of order $\kappa_D \lambda/(\beta e)$, reads

$$\Phi^{\text{qu}(\kappa_D \lambda)}(x) = -\hbar \mathcal{B} e^{-\kappa_D x} \quad \text{with } \mathcal{B} = \frac{\pi}{\sqrt{2}} \frac{\sum_{\gamma} (e_{\gamma}/\sqrt{m_{\gamma}}) \rho_{\gamma}^B}{\sqrt{\sum_{\alpha} e_{\alpha}^2 \rho_{\alpha}^B}}. \quad (1.12)$$

$\Phi^{\text{qu}(\kappa_D \lambda)}(x)$ appears only when species have different masses, because of the bulk local neutrality

$$\sum_{\alpha} e_{\alpha} \rho_{\alpha}^B = 0. \quad (1.13)$$

The density profile (1.10) can be rewritten as

$$\rho_{\alpha}(x) = \left(1 - e^{-2x^2/\lambda_{\alpha}^2}\right) \left[\rho_{\alpha}^{\text{cl}(\varepsilon_D)}(x) + \hbar \rho_{\alpha}^B \beta e_{\alpha} \mathcal{B} e^{-\kappa_D x}\right] + \rho_{\alpha}^B o(\varepsilon_D, \kappa_D \lambda), \quad (1.14)$$

where $\rho_{\alpha}^{\text{cl}(\varepsilon_D)}(x)$ is the classical density profile calculated up to relative order ε_D [1] and written in (5.47). We stress that the direct contribution (1.2) from the vanishing of wave-functions in the ranges λ_{α} 's from the wall has an essential singularity in \hbar , whereas the quantum part of the electrostatic potential at leading order, $\Phi^{\text{qu}(\kappa_D \lambda)}(x)$, is linear in \hbar . (We recall that for systems invariant under translations – which is not the case here – and with sufficiently smooth potentials – such as the Coulomb interaction – \hbar -expansions involve only even powers of \hbar , as can be seen for instance in Wigner-Kirkwood expansions.)

The appearance in the electrostatic potential $\Phi(x)$ of a \hbar -term which decays exponentially fast over the classical Debye screening length ξ_D has the following physical interpretation. When species have different masses, the global charge $\sigma_{<}$ carried by the fluid (per unit area) over all distances $x < a$ from the wall is essentially created at leading order by the differences in the Gaussian density profiles and is concentrated over a width of order λ . Since λ is negligible with respect to the bulk mean interparticle distance a , the leading-order charge $\sigma_{<}^{\text{qu}(\kappa_D \lambda)}$ can be seen as a surface charge localized at $x = 0$. As shown in Section 6.4, the surface charge $\sigma_{<}^{\text{qu}(\kappa_D \lambda)}$, which appears even in the zero-coupling limit, creates an electrostatic potential through the classically-screened Coulomb interaction (calculated at leading order), and this potential is equal to the leading \hbar -term $\Phi^{\text{qu}(\kappa_D \lambda)}(x)$ in the electrostatic potential $\Phi(x)$ created by the charge-density profile $\sum_{\alpha} e_{\alpha} \rho_{\alpha}(x)$. Moreover $\Phi^{\text{qu}(\kappa_D \lambda)}(x)$ is involved in the density profiles in such a way that the leading-order global charge $\sigma_{>}^{\text{qu}(\kappa_D \lambda)}$ carried by the fluid (per unit area) over all distances $x > a$, and which is dilute over the scale ξ_D , compensates $\sigma_{<}^{\text{qu}(\kappa_D \lambda)}$ (see Section 6.4). Indeed, since the wall is made of an insulating material and carries no external charge, the global surface charge σ carried

by the fluid per unit area vanishes at equilibrium [2]

$$\sigma \equiv \int_0^\infty dx \sum_\alpha e_\alpha \rho_\alpha(x) = 0. \quad (1.15)$$

$\sigma_{<}^{\text{qu}(\kappa_D \lambda)}$ and $\Phi^{\text{qu}(\kappa_D \lambda)}(x=0)$ are estimated in the case of the intrinsic semiconductor GaSb. The case where the wall has not the same dielectric constant as the medium where the fluid is embedded is commented in Section 7.

1.3 Methods

Before going into details, we summarize the general methods displayed in Sections 2–5.

First, a formalism based on path integrals and devised for the study of bulk properties in Coulomb fluids – with Maxwell-Boltzmann statistics [3] then quantum statistics [4]– is generalized to a semi-infinite geometry (Section 2). The system is studied in the grand-canonical ensemble (Section 2.1). A degeneracy of physical quantities with respect to fugacities arises from the neutrality constraints enforced by the long-range of Coulomb interactions. We investigate the nature of this degeneracy, and we show that we are allowed to split the latter degeneracy in order to impose the local neutrality in the zero-coupling limit (Section 2.2). (This trick allows to simplify weak-coupling expansions performed in Section 5.) By use of the Feynman-Kac formula (Section 2.3), quantum dynamics can be described by a functional integral over Brownian paths, which correspond to quantum position fluctuations. As in the bulk situation, the quantum system of point charges is equivalent to a classical system of loops with random shapes (Section 2.4). The only difference in formulae for the bulk or for the vicinity of the wall is that the path measure is anisotropic and depends on the distance from the wall in the second case.

Then methods originally devised for classical fluids with internal degrees of freedom can be used (Section 3). In Section 3.1 we introduce generalized Mayer diagrams for the fugacity expansion of the loop density of each species. Point weights in those diagrams depend both on the internal degrees of freedom of loops – charge and shape – and on the distance x from the wall. Because of the long range of Coulomb interaction, every Mayer diagram that is not sufficiently connected corresponds to a divergent integral in the thermodynamical limit. These divergences disappear after exact systematic resummations analogous to those performed in Ref.[4] (Section 3.2). (Details are provided in Appendix A.) Resummations introduce a screened potential $\phi(\mathbf{r}, \mathbf{r}')$, solution of an inhomogeneous Debye equation

$$[\Delta_{\mathbf{r}} - \bar{\kappa}^2(x)] \phi(\mathbf{r}, \mathbf{r}') = -4\pi\delta(\mathbf{r} - \mathbf{r}'), \quad (1.16)$$

where the effective screening length $1/\bar{\kappa}(x)$ depends on the distance x to the wall because of the vanishing of wave-functions at the wall surface (see (1.2)).

At this point the difficulty to be circumvented is the resolution of equation (1.16) (Section 4). The equation can be turned into a one-dimensional differential equation by considering the Fourier transform $\phi(x, x', \mathbf{k})$ of $\phi(x, x', \mathbf{y})$ in the directions parallel to the wall surface (Section 4.1). Let $\phi^{(0)}(x, x', \mathbf{y})$ be the expression that $\phi(x, x', \mathbf{y})$ would take if the profile $\bar{\kappa}(x)$ were uniform and equal to its bulk value κ in the region $x > 0$. A formal series representation of the solution $\phi(x, x', \mathbf{k}) - \phi^{(0)}(x, x', \mathbf{k})$ has been given in Ref. [5], where a similar equation arises in the case of a classical charge fluid in the vicinity of a wall with an electrostatic response. This series provides an expansion of the solution $\phi(x, x', \mathbf{k})$ around $\phi^{(0)}(x, x', \mathbf{k})$ in powers of the small parameter $\kappa\lambda$, where κ is the limit of $\bar{\kappa}(x)$ when x goes to infinity, while λ is the length scale over which $\bar{\kappa}(x)$ varies quickly when x approaches 0. The expansion of $\phi(x, x', \mathbf{k}) - \phi^{(0)}(x, x', \mathbf{k})$ in powers of $\kappa\lambda$ is uniform in x and x' .

In the low-degeneracy and weak-coupling regime to be studied (Section 5.1), the condition $\kappa\lambda \ll 1$ is met. The screened self-energy is purely classical at leading order and the quantum correction appears only at order $\varepsilon \times \kappa\lambda$, where ε is defined as ε_D with κ in place of κ_D , $\varepsilon \equiv (1/2)\kappa\beta e^2$ (Section 5.2). A scaling analysis performed in the low-degeneracy and weak-coupling limit (Section 5.3 and Appendix B) shows that only one resummed Mayer diagram contributes to density profiles at first order in ε and $\kappa\lambda$. The electrostatic potential drop $\Phi(x)$ created by the charge-density profile is identified in the formal expression of the contribution from this diagram (Section 5.4). Because of the local neutrality condition in the bulk, only the classical zeroth-order term in the $\kappa\lambda$ -expansion of $\phi - \phi^{(0)}$ proves to contribute to the potential drop $\Phi(x)$ at leading orders ε and $\kappa\lambda$.

2 General formalism

2.1 Grand-canonical ensemble and statistics

We recall that we consider a fluid made of n_s species (indexed by α), each of which is characterized by its mass m_α , its charge e_α , and its spin $S_\alpha\hbar$. (In the following, interactions involving spins will be neglected and spin will only determine the nature of quantum statistics.) The Hamiltonian operator $\hat{H}_{\{N_\alpha\}}$ of a system which contains N_α particles of each species α reads

$$\hat{H}_{\{N_\alpha\}} = \sum_i \frac{\hat{\mathbf{p}}_i^2}{2m_{\alpha_i}} + \sum_i \widehat{V_{SR}}(x_i) + \sum_{i < j} e_{\alpha_i} e_{\alpha_j} \widehat{v}(\mathbf{r}_i - \mathbf{r}_j). \quad (2.1)$$

($\{N_\alpha\}$ is a shorthand notation for $\{N_\alpha\}_{\alpha=1,\dots,n_s}$ and the particle index i runs from 1 to $N = \sum_\alpha N_\alpha$.) In (2.1) the first term which involves the momentum operator $\widehat{\mathbf{p}}$ is the global kinetic energy of the system. The second term is a sum of one-body potentials $\widehat{V}_{SR}(x_i)$ which describe the particle-wall interactions. We choose a simple classical hard-wall modelization, where the atomic structure of the wall is ignored. The effect of the wall is only to prevent particle wave-functions from propagating inside the negative- x region occupied by the wall,

$$V_{SR}(x) = \begin{cases} +\infty & \text{if } x < 0 \\ 0 & \text{if } x > 0. \end{cases} \quad (2.2)$$

The wall repulsion is independent of the particle species. The sum of pair interactions in the third term involves only Coulomb potential (1.1).

The fixed parameters of the system are the volume $|\Lambda|$ of the region Λ that the fluid occupies, the area $|\partial_w \Lambda|$ of the fluid-wall interface, the temperature, and the densities ρ_α^B 's far away from the boundaries of Λ . We use the grand-canonical ensemble where the parameters are the volume $|\Lambda|$, the area $|\partial_w \Lambda|$, the inverse temperature β , and the chemical potentials $\{\mu_\alpha(V_R)\}_{\alpha=1,\dots,n_s}$ of particles in a reservoir where the electrostatic potential takes the uniform value V_R . The grand partition function reads

$$\Xi(\beta, \{\mu_\alpha\}, |\Lambda|, |\partial_w \Lambda|) = \sum_{\{N_\alpha\}} \text{Tr}_{\Lambda, \{N_\alpha\}}^{\text{sym}} e^{-\beta[\widehat{H}_{\{N_\alpha\}} - \sum_\alpha \mu_\alpha \widehat{N}_\alpha]}, \quad (2.3)$$

where the trace $\text{Tr}_{\Lambda, \{N_\alpha\}}^{\text{sym}}$ is restricted to the quantum states that are properly symmetrized according to the Bose-Einstein or Fermi-Dirac statistics obeyed by each species. (\widehat{N}_α is the particle-number operator for species α .) As in the classical case, the density profile $\rho_\alpha(x)$ can be determined by using a functional derivation of $\Xi[\widetilde{\mu}_\alpha]$, where $\sum_\alpha \mu_\alpha \widehat{N}_\alpha$ is replaced by $\int_\Lambda d\mathbf{r} \widetilde{\mu}_\alpha(x) \widehat{\rho}_\alpha(x)$. The relation is

$$\rho_\alpha(x) = \lim_{|\Lambda| \rightarrow +\infty} \frac{1}{\beta} \left. \frac{\delta \ln \Xi[\widetilde{\mu}_\alpha]}{\delta \widetilde{\mu}_\alpha(x)} \right|_{\widetilde{\mu}_\alpha(x) = \mu_\alpha}. \quad (2.4)$$

The formalism and results presented in Sections 2 and 3 can be obtained with quantum statistics (as detailed in Section 2.4). However, our aim is to produce explicit analytical results in the low-degeneracy regime (1.4). We have checked that quantum statistics effects arise only at order $(\lambda/a)^3$. In other words [3]

$$\Xi = \Xi_{\text{MB}} + \mathcal{O}\left(\left(\frac{\lambda}{a}\right)^3\right), \quad (2.5)$$

where the Maxwell-Boltzmann grand partition function Ξ_{MB} is a trace over tensorial products of one-particle wavefunctions which are not symmetrized

according to species statistics. If the tensorial product of $N = \sum_{\alpha} N_{\alpha}$ one-particle states in position representation is denoted by $|\{\mathbf{r}_i\}\rangle$, the grand partition function Ξ_{MB} , where only dynamics is quantum, reads

$$\begin{aligned} \Xi_{\text{MB}}(\beta, \{\mu_{\alpha}\}, |\Lambda|, |\partial_w \Lambda|) \\ = \sum_{\{N_{\alpha}\}} \left[\prod_{\alpha} \frac{e^{\beta \mu_{\alpha} N_{\alpha}} (2S_{\alpha} + 1)^{N_{\alpha}}}{N_{\alpha}!} \right] \int \left[\prod_{i=1}^N d\mathbf{r}_i \right] \langle \{\mathbf{r}_i\} | e^{-\beta \hat{H}_{\{N_{\alpha}\}}} | \{\mathbf{r}_i\} \rangle. \end{aligned} \quad (2.6)$$

where $2S_{\alpha} + 1$ is the spin degeneracy factor, which arises because spin does not appear in the expression (2.1) of the Hamiltonian. In (2.6) we have used the commutativity of the operators $\hat{H}_{\{N_{\alpha}\}}$ and \hat{N}_{α} 's.

2.2 Degeneracy with respect to fugacities

In the following we will take advantage of a degeneracy of physical quantities with respect to fugacities that arises from the vanishing of the global volumic and surfacic charges of the system in the thermodynamic limit. If $\langle \cdots \rangle$ denotes a grand-canonical average, the thermodynamic limit of the charge in the fluid is

$$\lim_{\text{th}} \langle \sum_{\alpha} e_{\alpha} N_{\alpha} \rangle = \left(\sum_{\alpha} e_{\alpha} \rho_{\alpha}^B \right) |\Lambda| + \sigma |\partial_w \Lambda| + o(|\partial_w \Lambda|), \quad (2.7)$$

where $o(|\partial_w \Lambda|)$ denotes a term which diverges more slowly than the area $|\partial_w \Lambda|$ when the size of the domain Λ becomes infinite. The expression of σ in terms of the thermodynamic limits of density profiles is given in (1.15). As a consequence of the existence of the thermodynamical limit [6], the macroscopic volumic charge $(\sum_{\alpha} e_{\alpha} \rho_{\alpha}^B) |\Lambda|$ vanishes, and, in the case of an insulating hard wall that is not externally charged, the surfacic charge in the fluid $\sigma |\partial_w \Lambda|$ is also equal to zero (whether the dielectric constants in the wall and in the medium where the fluid is embedded are equal or not). Indeed, in the grand canonical ensemble (2.3), the summation over microscopic states involves non-neutral configurations, but the self-energies of these globally charged configurations give them exponentially vanishing weights in the thermodynamic limit, because they are not compensated by interaction energies with external charges inside the walls.

Since the bulk charge neutrality (1.13) is satisfied for any set of chemical potentials, the bulk densities ρ_{α}^B 's are determined by only $n_s - 1$ independent functions of the n_s chemical potentials μ_{α} 's. In the present paragraph we investigate more precisely the nature of the corresponding degeneracy.

By definition, the electrostatic energy in the Hamiltonian (2.1) used in Ξ (2.3) is the difference between the electrostatic energy of the interacting

system and the energy $V_R \sum_{\alpha} e_{\alpha} N_{\alpha}$ of the noninteracting system in the reservoir where the electrostatic potential takes the uniform value V_R . In other words, the dependence of chemical potentials with respect to the potential V_R in the reservoir is just

$$\mu_{\alpha}(V_R) = \mu_{\alpha}(0) + e_{\alpha} V_R. \quad (2.8)$$

The global volumic and surfacic neutralities are linked to the invariance of the thermodynamic limits of observables under a translation of the origin for the electrostatic potentials. Indeed, if the latter origin is translated by an amount $-\Delta V$, then, the reference potential V_R of the reservoir becomes $V_R + \Delta V$, the Hamiltonian is unchanged (since the insulating wall carries no external charge), and the only change in Ξ (2.3) is an extra contribution $\Delta V \sum_{\alpha} e_{\alpha} N_{\alpha}$ arising from $\sum_{\alpha} \mu_{\alpha}(V_R) N_{\alpha}$. Then the thermodynamic limit of $\ln \Xi$ is increased by

$$\Delta \left(\lim_{\text{th}} \ln \Xi \right) = \beta \Delta V \lim_{\text{th}} \left\langle \sum_{\alpha} e_{\alpha} N_{\alpha} \right\rangle \quad (2.9)$$

According to (2.7), (1.13), and (1.15), the latter variation vanishes up to order $|\partial_w \Lambda|$ included.

Since a translation $-\Delta V$ of the origin for the electrostatic potentials is equivalent to an increase $e_{\alpha} \Delta V$ of every μ_{α} , the nature of the degeneracy of physical quantities with respect to chemical potentials is that physical quantities are invariant under the addition of an energy $e_{\alpha} \Delta V$ to every chemical potential μ_{α} . The corresponding degeneracy with respect to fugacities z_{α} 's comes from the definition

$$z_{\alpha}(V_R) \equiv \frac{(2S_{\alpha} + 1)}{(2\pi\lambda_{\alpha}^2)^{3/2}} \exp[\beta\mu_{\alpha}(V_R)], \quad (2.10)$$

The dependence of fugacities upon V_R is given by (2.8). The system involves charges of both signs, so that the continuous function $f(V_R) = \sum_{\alpha} e_{\alpha} z_{\alpha}(V_R)$ varies from $-\infty$ up to $+\infty$ when V_R varies from $-\infty$ to $+\infty$. Therefore there exists a value of V_R which fulfills the condition $f(V_R) = 0$.

As a consequence, since physical quantities are invariant under a translation of V_R in the fugacities, we can choose a set of fugacities which ensures that the local charge neutrality in the bulk is enforced even in the zero-coupling limit, namely we can arbitrarily split the degeneracy with respect to fugacities by imposing

$$\sum_{\alpha} e_{\alpha} z_{\alpha} = 0. \quad (2.11)$$

We notice that, as shown in Ref.[7], in the case of an insulating wall with an external charge or in the case of a conducting wall, which becomes charged

by influence, the global neutrality of the full system (the fluid plus the wall) in the thermodynamic limit implies that condition (2.11) can also be fulfilled when Ξ is written with the full Hamiltonian. The “neutrality” condition about fugacities (2.11) will cause major simplifications in the following calculations.

2.3 Feynman-Kac formula

The non-commutativity between the kinetic and interaction operators in (2.6) can be circumvented by using Feynman-Kac formula [8, 9]. The quantum Gibbs factor can be rewritten in terms of path integrals,

$$\begin{aligned} \langle \{\mathbf{r}_i\} | e^{-\beta \hat{H}_{\{N\alpha\}}} | \{\mathbf{r}_i\} \rangle &= \left[\prod_i \frac{1}{(2\pi\lambda_{\alpha_i}^2)^{3/2}} \right] \int \left[\prod_i \mathcal{D}_{x_i, \alpha_i}(\boldsymbol{\xi}_i) \right] \\ &\times \exp \left[-\beta \sum_{i < j} e_{\alpha_i} e_{\alpha_j} \int_0^1 ds v(\mathbf{r}_i + \lambda_{\alpha_i} \boldsymbol{\xi}_i(s) - \mathbf{r}_j - \lambda_{\alpha_j} \boldsymbol{\xi}_j(s)) \right]. \end{aligned} \quad (2.12)$$

The kinetic part of the Hamiltonian and the particle-wall interaction are taken into account in the measure $\mathcal{D}_{x_i, \alpha_i}(\boldsymbol{\xi}_i)$ of the closed Brownian path $\boldsymbol{\xi}_i$ with dimensionless abscissa s : $\boldsymbol{\xi}(s=0) = \boldsymbol{\xi}(s=1) = \mathbf{0}$. The random path $\lambda_{\alpha_i} \boldsymbol{\xi}_i(s)$ with typical extent λ_{α_i} describes the quantum position fluctuations of particle i at position \mathbf{r}_i . As discussed in Section 2.4, the interaction between paths on the r.h.s. of (2.12) is not the usual Coulomb interaction between charged wires, since it involves only path elements with the same abscissa s .

The repulsion from the wall causes the anisotropy of the Brownian-path measure. The constraint about the quantum particle position, which is described by $V_{SR}(x)$, enforces that the x -component ξ_x of vector $\boldsymbol{\xi}$ obeys the inequality

$$x + \lambda_{\alpha} \xi_x(s) > 0 \quad (2.13)$$

for every s between 0 and 1. The Brownian path measure can be factorized as

$$\mathcal{D}_{x, \alpha}(\boldsymbol{\xi}) = \mathcal{D}_{x, \alpha}(\xi_x) \mathcal{D}(\boldsymbol{\xi}_{\parallel}), \quad (2.14)$$

where $\boldsymbol{\xi}_{\parallel}$ is the projection of $\boldsymbol{\xi}$ onto the wall. As in the bulk, the Gaussian measure $\mathcal{D}(\boldsymbol{\xi}_{\parallel})$ is independent of the position \mathbf{r} . Moreover it is rotational-invariant and normalized to unity

$$\int \mathcal{D}(\boldsymbol{\xi}_{\parallel}) = 1. \quad (2.15)$$

On the contrary, as recalled in Ref. [10], the measure $\mathcal{D}_{x,\alpha}(\xi_x)$ depends on x , with for instance

$$\int \mathcal{D}_{x,\alpha}(\xi_x) = 1 - e^{-2x^2/\lambda_\alpha^2}. \quad (2.16)$$

Moreover, the mean extent of the path in the x -direction does not vanish

$$\int \mathcal{D}_{x,\alpha}(\xi_x) \xi_x \neq 0. \quad (2.17)$$

All moments of the measure tend gaussianly fast to their bulk values over the scale of the de Broglie wavelengths. For instance

$$\int_0^1 ds \int \mathcal{D}_{x,\alpha}(\xi_x) \xi_x(s) = \sqrt{\frac{\pi}{2}} \left(\frac{x}{\lambda_\alpha} \right)^2 \text{Erfc} \left(\sqrt{2} \frac{x}{\lambda_\alpha} \right), \quad (2.18)$$

where $\text{Erfc}(u)$ is the complementary error function defined as

$$\text{Erfc}(u) = \frac{2}{\sqrt{\pi}} \int_u^\infty dt e^{-t^2}. \quad (2.19)$$

$\text{Erfc}(u)$ decays as $\exp[-u^2]/(u\sqrt{\pi})$ when u goes to $+\infty$.

2.4 Equivalence with a classical gas of loops

In the present paragraph we recall that the quantum grand partition function Ξ for point particles can be written as a classical grand partition function Ξ_{loop} for randomly shaped loops [4]. The latter formalism including quantum statistics allows one to retrieve property (2.5) : quantum statistics effects appear only at order $(\lambda/a)^3$ in the low-degeneracy regime. In other words, results at leading order in the low-degeneracy regime (1.4) are the same when the starting partition function is written with Maxwell-Boltzmann statistics. Therefore, for the sake of simplicity, we shall directly consider Ξ_{MB} and we shall drop the index MB from now on.

The quantum grand partition function (2.6) can be rewritten by use of the Feynman-Kac formula (2.12) as

$$\begin{aligned} \Xi(\beta, \{z_\alpha\}, \Lambda) = \Xi_{\text{loop}} &\equiv \sum_{N=0}^{\infty} \frac{1}{N!} \int \left[\prod_{n=1}^N d\mathcal{L}_n z(\mathcal{L}_n) \right] \\ &\times \exp \left[-\beta \sum_{i < j} e_{\alpha_i} e_{\alpha_j} \mathcal{V}(\mathcal{L}_i, \mathcal{L}_j) \right]. \end{aligned} \quad (2.20)$$

In (2.20) the notation $\mathcal{L} \equiv (\mathbf{r}, \boldsymbol{\xi}, \alpha)$ stands for the loop position \mathbf{r} , the loop shape $\boldsymbol{\xi}$ and the loop species α . When the measure is defined as

$$\int d\mathcal{L} \equiv \sum_{\alpha=1}^{n_s} \int_{\Lambda} d\mathbf{r} \int \mathcal{D}_{x,\alpha}(\boldsymbol{\xi}), \quad (2.21)$$

simple combinatorics allows one to replace the summation over the N_α 's by a single summation over $N = \sum_{\alpha} N_\alpha$. The loop fugacity depends on the distance from the wall as

$$z(\mathcal{L}) = z_\alpha \theta(x), \quad (2.22)$$

where $\theta(x)$ is the unit Heaviside function. The interaction between loops arising from the Feynman-Kac formula couples only line elements with the same abscissa s

$$\mathcal{V}(\mathcal{L}_i, \mathcal{L}_j) \equiv \int_0^1 ds v(\mathbf{r}_i + \lambda_{\alpha_i} \boldsymbol{\xi}_i(s) - \mathbf{r}_j - \lambda_{\alpha_j} \boldsymbol{\xi}_j(s)). \quad (2.23)$$

Thus it is different from the electrostatic potential $\mathcal{V}_{\text{elect}}(\mathcal{L}_i, \mathcal{L}_j)$ between uniformly charged wires where any line element of a loop interacts with every line element of the other loop,

$$\mathcal{V}_{\text{elect}}(\mathcal{L}_i, \mathcal{L}_j) \equiv \int_0^1 ds \int_0^1 ds' v(\mathbf{r}_i + \lambda_{\alpha_i} \boldsymbol{\xi}_i(s) - \mathbf{r}_j - \lambda_{\alpha_j} \boldsymbol{\xi}_j(s')). \quad (2.24)$$

For a system with quantum statistics, Ξ_{loop} has the general expression written in (2.20) where loops \mathcal{L} and their fugacities $z(\mathcal{L})$ have more complex expressions than in the case of Maxwell-Boltzmann statistics [4]. Quantum statistics is taken into account thanks to an extra internal degree of freedom, the number of particles exchanged in the same permutation cycle.

Equality (2.20) between the grand partition function of a quantum gas of point particles and the grand partition function of a classical system of loops with random shapes is the root of an equivalence between both systems. As derived in Ref.[4], the quantum density $\rho_\alpha(x)$ can be determined from the loop density $\rho(\mathcal{L})$ defined as a grand-canonical average calculated with Ξ_{loop} . When exchange effects are neglected,

$$\rho(\mathcal{L}) \equiv \left\langle \sum_n \delta(\mathbf{r}_n - \mathbf{r}) \delta(\boldsymbol{\xi}_n - \boldsymbol{\xi}) \delta_{\alpha_n, \alpha} \right\rangle_{\Xi_{\text{loop}}}, \quad (2.25)$$

and the relation between particle and loop densities reads

$$\rho_\alpha(x) = \int \mathcal{D}_{x,\alpha}(\boldsymbol{\xi}) \rho(\mathcal{L}), \quad (2.26)$$

where $\rho(\mathcal{L})$, with $\mathcal{L} = (\mathbf{r}, \boldsymbol{\xi}, \alpha)$, does not depend on the projection \mathbf{y} of \mathbf{r} onto the wall plane.

2.5 Ideal gas

In the case of an ideal quantum gas, the grand partition function (2.20) is reduced to

$$\Xi^{\text{id}} = \exp \left\{ \sum_{\alpha} z_{\alpha} \int_{\Lambda} d\mathbf{r} \int \mathcal{D}_{x,\alpha}(\xi) \right\} + \mathcal{O} \left(\left(\frac{\lambda_{\alpha}}{a_{\alpha}} \right)^3 \right), \quad (2.27)$$

and, by virtue of (2.25), $\rho^{\text{id}}(\mathcal{L}) = z(\mathcal{L})$ given in (2.22). The density profiles of an ideal gas with fugacities z_{α} 's are given by (2.4) (or equivalently by (2.26)), and by using (2.14)–(2.16) we retrieve that

$$\rho_{\alpha}^{\text{id}}(x) = z_{\alpha} \left[1 - e^{-2x^2/\lambda_{\alpha}^2} \right] + z_{\alpha} \mathcal{O} \left(\left(\frac{\lambda_{\alpha}}{a_{\alpha}} \right)^3 \right). \quad (2.28)$$

We stress that, in the vicinity of the wall, the quantum charge fluid cannot be handled with as a system made of independent charges, because it cannot simultaneously obey the volumic global neutrality (1.13) and the surfacic global neutrality (1.15). Indeed, the bulk densities in the ideal gas are equal to the z_{α} 's. If the constraint (2.11) is arbitrarily enforced upon fugacities, though there is no degeneracy with respect to fugacities in the purely noninteracting case, the bulk densities satisfy the bulk local neutrality relation (1.13). However, the global surface charge of the corresponding ideal gas does not vanish when species have different masses: according to (2.11) and (2.28), it is equal to

$$\sigma^{\text{id}} \equiv \int_0^{\infty} dx \sum_{\alpha} e_{\alpha} \rho_{\alpha}^{\text{id}}(x) = -\frac{1}{2} \sqrt{\frac{\pi}{2}} \sum_{\alpha} e_{\alpha} z_{\alpha} \lambda_{\alpha}. \quad (2.29)$$

3 Diagrammatic representation

The main lines of the following diagrammatic expansions are analogous to the formalisms devised for bulk quantum properties and classical density profiles in Refs. [4] and [5], respectively.

3.1 Generalized fugacity-expansions

The equivalence with the classical loop system allows one to use techniques originally introduced for classical fluids. For instance, the Mayer diagrammatics initially built for point particles can be generalized to objects with internal degrees of freedom, such as the species α or the loop shape ξ . A generalized Mayer diagram for the loop density $\rho(\mathcal{L})$ contains one root point \mathcal{L} which is not integrated over and N internal points ($N = 1, \dots, \infty$)

which are integrated over, while each pair of points is linked by at most one bond

$$f(\mathcal{L}_i, \mathcal{L}_j) = e^{-\beta e_{\alpha_i} e_{\alpha_j} \mathcal{V}(\mathcal{L}_i, \mathcal{L}_j)} - 1. \quad (3.1)$$

We choose to write the loop-fugacity expansion of the loop density as

$$\rho(\mathcal{L}) = z(\mathcal{L}) \exp \left\{ \sum_{\mathbb{G}} \frac{1}{S_{\mathbb{G}}} \int \left[\prod_{n=1}^N d\mathcal{L}_n z(\mathcal{L}_n) \right] [\prod f]_{\mathbb{G}} \right\}. \quad (3.2)$$

The summation is performed over all unlabeled, topologically different, connected diagrams \mathbb{G} where the root point \mathcal{L} is not an articulation point. An articulation point is defined by the following property: if it is taken out of the diagram, the latter is split into at least two pieces not linked together by any bond. (In another diagrammatic representation [4], which is analogous to (3.2) but without the exponential, the root point \mathcal{L} may be an articulation point.) $[\prod f]_{\mathbb{G}}$ is the product of the f -bonds in diagram \mathbb{G} and $S_{\mathbb{G}}$ is the symmetry factor, i.e. the number of permutations of internal points \mathcal{L}_n that do not change this product.

$$\rho(\mathcal{L}) = z(\mathcal{L}) \exp \left\{ \mathcal{L} \text{---} \text{---} \text{---} \text{---} z + \mathcal{L} \text{---} \text{---} \text{---} \text{---} z \text{---} z + \mathcal{L} \text{---} \text{---} \text{---} \text{---} \begin{array}{c} z \\ f \\ f \\ z \end{array} + \dots \right\}$$

Figure 1: Mayer diagrammatic representation of the loop density. A white point stands for the root loop of the diagram, the coordinates of which are not integrated over. Black points are internal loop-points, the coordinates of which are integrated over. The f -bond between two loops is represented by a line and the weight of a black point associated with a loop \mathcal{L}_i is the loop fugacity $z(\mathcal{L}_i)$.

At large distances with respect to de Broglie thermal wavelengths, the loop potential $\mathcal{V}(\mathcal{L}, \mathcal{L}')$ behaves as the Coulomb potential between the total charges of loops, as if they were concentrated at positions \mathbf{r} and \mathbf{r}' . Because of the latter $1/|\mathbf{r} - \mathbf{r}'|$ interactions, the integrals associated with generic diagrams \mathbb{G} in (3.2) diverge in the thermodynamical limit.

3.2 Systematic resummations of large-distance Coulomb divergences

The large-distance divergences arising from the long-range of Coulomb potential can be dealt with by introducing auxiliary bonds and by systematically resumming subclasses of auxiliary diagrams $\tilde{\mathbb{G}}$. The method is a

generalization of the procedure introduced by Meeron for bulk quantities in a classical Coulomb fluid [11]. The systematic resummation procedure is displayed in Appendix A where similarities and differences with the process used in Ref.[4] are stressed.

As in Ref.[4], the decomposition into auxiliary bonds relies on the multipolar decomposition of the loop interaction. This decomposition allows one to exhibit classical screening through the appearance of a screened potential ϕ arising from the resummation process. It reads

$$\mathcal{V}(\mathcal{L}_i, \mathcal{L}_j) = \mathcal{V}^{\text{cc}}(\mathbf{r}_i - \mathbf{r}_j) + \mathcal{V}^{\text{cm}}(\mathbf{r}_i, \mathcal{L}_j) + \mathcal{V}^{\text{mc}}(\mathcal{L}_i, \mathbf{r}_j) + \mathcal{V}^{\text{mm}}(\mathcal{L}_i, \mathcal{L}_j). \quad (3.3)$$

where $\mathcal{V}^{\text{cc}}(\mathbf{r}_i - \mathbf{r}_j) = v(\mathbf{r}_i - \mathbf{r}_j)$ is the charge-charge – i.e. monopole-monopole – interaction between the total loop charges, and the charge-multipole interaction \mathcal{V}^{cm} is equal to

$$\mathcal{V}^{\text{cm}}(\mathbf{r}_i, \mathcal{L}_j) \equiv \int_0^1 ds \left[v(\mathbf{r}_i - \mathbf{r}_j - \lambda_{\alpha_j} \boldsymbol{\xi}_j(s)) - v(\mathbf{r}_i - \mathbf{r}_j) \right], \quad (3.4)$$

with a symmetric definition for \mathcal{V}^{mc} . The multipole-multipole interaction \mathcal{V}^{mm} is

$$\begin{aligned} \mathcal{V}^{\text{mm}}(\mathcal{L}_i, \mathcal{L}_j) &= \mathcal{V}(\mathcal{L}_i, \mathcal{L}_j) - v(\mathbf{r}_i - \mathbf{r}_j) - \mathcal{V}^{\text{cm}}(\mathbf{r}_i, \mathcal{L}_j) - \mathcal{V}^{\text{mc}}(\mathcal{L}_i, \mathbf{r}_j) \\ &= \int_0^1 ds \left[v(\mathbf{r}_i + \lambda_i \boldsymbol{\xi}_i(s) - \mathbf{r}_j - \lambda_j \boldsymbol{\xi}_j(s)) - v(\mathbf{r}_i + \lambda_i \boldsymbol{\xi}_i(s) - \mathbf{r}_j) \right. \\ &\quad \left. - v(\mathbf{r}_i - \mathbf{r}_j - \lambda_j \boldsymbol{\xi}_j(s)) + v(\mathbf{r}_i - \mathbf{r}_j) \right]. \end{aligned} \quad (3.5)$$

\mathcal{V}^{cm} does coincide with the charge-multipole Coulomb interaction between a point charge and a charged wire, whereas \mathcal{V}^{mm} is not equal to the multipole-multipole Coulomb interaction between two charged wires, because it couples only line elements of \mathcal{L} and \mathcal{L}' with the same abscissa. The resummation procedure introduces a screened potential ϕ arising from the sum of all chains built with the auxiliary bond $f^{\text{cc}}(\mathcal{L}, \mathcal{L}') = -\beta e_{\alpha} e_{\alpha'} v(\mathbf{r} - \mathbf{r}')$ (see Fig.2). It reads

$$\begin{aligned} -\beta e_{\alpha} e_{\alpha'} \phi(\mathbf{r}, \mathbf{r}') &= f^{\text{cc}}(\mathcal{L}, \mathcal{L}') \\ &+ \sum_{N=1}^{\infty} \int \left[\prod_{n=1}^N d\mathcal{L}_n z(\mathcal{L}_n) \right] f^{\text{cc}}(\mathcal{L}, \mathcal{L}_1) f^{\text{cc}}(\mathcal{L}_1, \mathcal{L}_2) \dots f^{\text{cc}}(\mathcal{L}_N, \mathcal{L}'). \end{aligned} \quad (3.6)$$

The properties of ϕ are studied hereafter.

When resummed bonds are defined, associated resummed weights and “excluded-composition” rules ensure a one-to-one correspondence between each class in the partition of auxiliary diagrams $\tilde{\mathbb{G}}$ and each resummed

$$\begin{aligned}
-\beta e_\alpha e_{\alpha'} \phi(\mathbf{r}, \mathbf{r}') &= \mathcal{L} \overset{F^{cc}}{\text{---}} \mathcal{L}' \\
&= \mathcal{L} \overset{f^{cc}}{\text{---}} \mathcal{L}' + \mathcal{L} \overset{f^{cc}}{\text{---}} \underset{z}{\bullet} \overset{f^{cc}}{\text{---}} \mathcal{L}' + \mathcal{L} \overset{f^{cc}}{\text{---}} \underset{z}{\bullet} \overset{f^{cc}}{\text{---}} \underset{z}{\bullet} \overset{f^{cc}}{\text{---}} \mathcal{L}' + \dots
\end{aligned}$$

Figure 2: Screened potential ϕ .

diagram \mathbb{P}^* . Contrary to what is done in Ref.[4], we choose to consider nine resummed bonds defined hereafter. The reason is that the choice of these nine bonds is associated with renormalized weights which are more convenient for dealing with the case of a wall with an electrostatic response (see Section 7) than the renormalized weights which appear when only the five resummed bonds of Ref.[4] are retained.

The nine resummed bonds are

$$F^{cc}(\mathcal{L}, \mathcal{L}') = -\beta e_\alpha e_{\alpha'} \phi(\mathbf{r}, \mathbf{r}'), \quad (3.7a)$$

$$F^{mc}(\mathcal{L}, \mathcal{L}') = -\beta e_\alpha e_{\alpha'} \int_0^1 ds \left[\phi(\mathbf{r} + \lambda_\alpha \boldsymbol{\xi}(s), \mathbf{r}') - \phi(\mathbf{r}, \mathbf{r}') \right] \quad (3.7b)$$

(see Fig.3) with a symmetric definition for F^{cm} , $(1/2)[F^{cc}]^2$ (see Fig.4), $(1/2)[F^{cm}]^2$, $(1/2)[F^{mc}]^2$, $F^{cc}.F^{cm}$, $F^{cc}.F^{mc}$, and

$$\begin{aligned}
F_{\text{RT}}(\mathcal{L}, \mathcal{L}') &= \left\{ e^{F^{cc} + F^{cm} + F^{mc} + F^{mm}} - 1 - F^{cc} - F^{cm} - F^{mc} \right. \\
&\quad \left. - \frac{1}{2}[F^{cc}]^2 - \frac{1}{2}[F^{cm}]^2 - \frac{1}{2}[F^{mc}]^2 - F^{cc}.F^{cm} - F^{cc}.F^{mc} \right\} (\mathcal{L}, \mathcal{L}').
\end{aligned} \quad (3.7c)$$

As shown in Ref.[4],

$$F^{mm}(\mathcal{L}, \mathcal{L}') = -\beta e_\alpha e_{\alpha'} \phi^{mm}(\mathcal{L}, \mathcal{L}') + W(\mathcal{L}, \mathcal{L}'), \quad (3.8)$$

where ϕ^{mm} is defined as \mathcal{V}^{mm} (3.5) with $\phi(\mathbf{r}, \mathbf{r}')$ in place of $v(\mathbf{r} - \mathbf{r}')$, and W is a purely quantum contribution,

$$\begin{aligned}
W(\mathcal{L}, \mathcal{L}') &= -\beta e_\alpha e_{\alpha'} [\mathcal{V}(\mathcal{L}, \mathcal{L}') - \mathcal{V}_{\text{elect}}(\mathcal{L}, \mathcal{L}')] \\
&= -\beta e_\alpha e_{\alpha'} \int_0^1 ds \int_0^1 ds' [\delta(s - s') - 1] \sum_{q=1}^{+\infty} \sum_{q'=1}^{+\infty} \frac{1}{q!} \frac{1}{q'!} \\
&\quad \times [\lambda_\alpha \boldsymbol{\xi}(s) \cdot \nabla_{\mathbf{r}}]^q [\lambda_{\alpha'} \boldsymbol{\xi}'(s') \cdot \nabla_{\mathbf{r}'}]^{q'} v(\mathbf{r} - \mathbf{r}').
\end{aligned} \quad (3.9)$$

We notice that the argument of the exponential in (3.7c) can be written $F^{cc} + F^{cm} + F^{mc} + F^{mm} = F_{\text{elect}} + W$, where $F_{\text{elect}} = -\beta e_\alpha e_{\alpha'} \int_0^1 ds \int_0^1 ds' \phi(\mathbf{r} + \lambda_\alpha \boldsymbol{\xi}(s), \mathbf{r}' + \lambda_{\alpha'} \boldsymbol{\xi}'(s'))$.

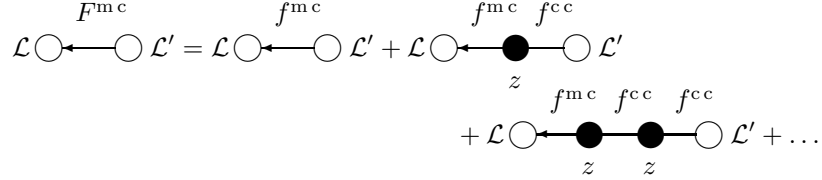


Figure 3: Resummed bond F^{mc} .

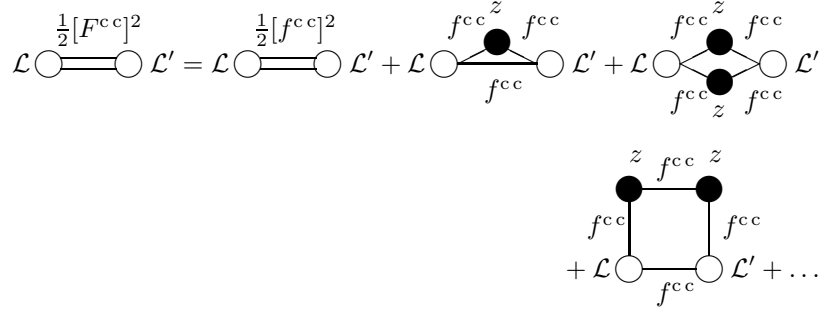


Figure 4: Resummed bond $\frac{1}{2} [F^{cc}]^2$. (The symmetry factors are not written in the figure.)

Eventually, the Mayer fugacity-expansion (3.2) of the loop density can be rewritten as

$$\rho(\mathcal{L}) = z^{\text{sc}}(\mathcal{L}) \exp \left\{ \sum_{\mathbb{P}^*} \frac{1}{S_{\mathbb{P}^*}} \int \left[\prod_{j=1}^N d\mathcal{L}_j w(\mathcal{L}_j) \right] [\prod F]_{\mathbb{P}^*} \right\}. \quad (3.10)$$

The effective screened fugacity arising from the resummation of Coulomb ring diagrams (defined in Appendix A and Fig.5) is equal to

$$z^{\text{sc}}(\mathcal{L}) = z(\mathcal{L}) e^{-\beta e_\alpha^2 \mathcal{V}_{\text{cloud}}^{\text{sc}}(\mathcal{L})}, \quad (3.11)$$

where $z(\mathcal{L}) = \theta(x) z_\alpha$ and

$$\mathcal{V}_{\text{cloud}}^{\text{sc}}(\mathcal{L}) = \frac{1}{2} \int_0^1 ds \int_0^1 ds' [\phi - v](\mathbf{r} + \lambda_\alpha \boldsymbol{\xi}(s), \mathbf{r} + \lambda_\alpha \boldsymbol{\xi}(s')). \quad (3.12)$$

The \mathbb{P}^* diagrams are defined as the \mathbb{G} diagrams in (3.2) apart from the following two differences. First the f -bond is replaced by the nine F -bonds. Second, \mathbb{P}^* diagrams obey an “excluded-composition” rule associated with the fact that all points have not the same weight $w(\mathcal{L})$ (in order to avoid double-counting),

$$w(\mathcal{L}) = \begin{cases} z^{\text{sc}}(\mathcal{L}) - z(\mathcal{L}) & \text{if } \mathcal{L} \text{ is involved only in a} \\ & \text{product } F^{\text{a c}}(\mathcal{L}_i, \mathcal{L}) F^{\text{c b}}(\mathcal{L}, \mathcal{L}_j) \\ z^{\text{sc}}(\mathcal{L}) & \text{otherwise.} \end{cases} \quad (3.13)$$

In (3.13) superscripts a and b stand either for c or m, and the points \mathcal{L}_i and \mathcal{L}_j may coincide.

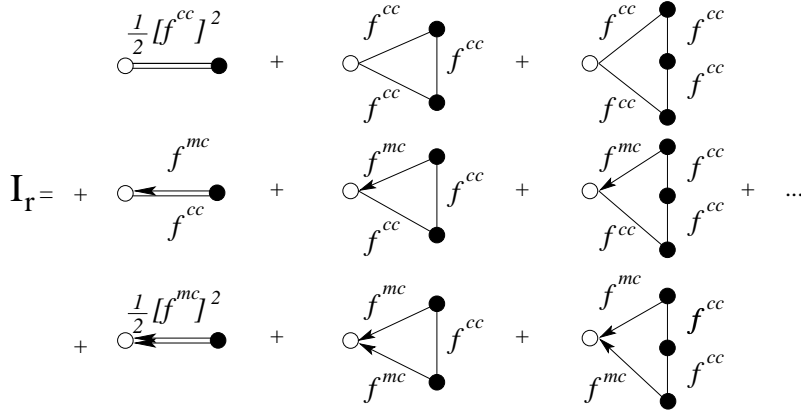


Figure 5: The sum of ring diagrams attached to a white point, $I_r = -\beta e_\alpha^2 \mathcal{V}_{\text{cloud}}^{\text{sc}}$.

The vicinity of the wall replaces the bulk exponential screening by an integrable algebraic screening in the directions parallel to the wall (see next section), and all diagrams with resummed bonds are finite in the thermodynamical limit, when integrations are performed first over loop shapes and then over loop positions. The reasons are the following ones. First, in $F^{\text{c c}}$ (3.7a) the resummed charge-charge interaction between the total loop charges is proportional to the screened potential $\phi(\mathbf{r}, \mathbf{r}')$ which obeys an inhomogeneous Debye equation where the screening length depends on the distance from the wall, as discussed in next section. The translational invariance along the wall ensures that $\phi(\mathbf{r}, \mathbf{r}') = \phi(x, x', \mathbf{y})$ where \mathbf{y} is the projection of $\mathbf{r} - \mathbf{r}'$ onto the wall. As shown in an analogous classical situation [12], where the inhomogeneity in the zero-coupling limit arises from the electrostatic response of the wall, when $|\mathbf{y}|$ goes to infinity while the

values of x and x' are kept fixed $\phi(\mathbf{r}, \mathbf{r}')$ decays as

$$\phi(\mathbf{r}, \mathbf{r}') \underset{|\mathbf{y}| \rightarrow +\infty}{\sim} \frac{f(x, x')}{|\mathbf{y}|^3}. \quad (3.14)$$

Far away from the wall the x -dependent screening length tends to a non-zero value, so that $f(x, x')$ decays exponentially fast to zero at large x or x' . Therefore the leading tail of F^{cc} has the structure $g^{cc}(x, x')/|\mathbf{y}|^3$ and F^{cc} is integrable. In F^{mc} (3.7b) the resummed multipole-charge interaction is also integrable. Indeed, since the Brownian path measure $\mathcal{D}_{x,\alpha}(\boldsymbol{\xi})$ ensures that all moments of $\boldsymbol{\xi}$ are finite, and the leading tail in F^{mc} , which is not canceled by the integration over the loop shape $\boldsymbol{\xi}$, behaves as

$$\int_0^1 ds \sum_{q=1}^{+\infty} \frac{1}{q!} [\lambda_\alpha \xi_x(s)]^q \frac{\partial^q g^{cc}(x, x')}{\partial x^q} \times \frac{1}{|\mathbf{y}|^3}. \quad (3.15)$$

$\partial^q g^{cc}(x, x')/\partial x^q$ is an exponentially vanishing function of x and x' far away from the wall, while $\int_0^1 ds \mathcal{D}_{x,\alpha}(\boldsymbol{\xi}) [\xi_x(s)]^q$ is a gaussianly vanishing function of x over the scale λ_α . As a consequence, the bond F^{cm} is also integrable in x and x' over the scales λ_α and $\lambda_{\alpha'}$, respectively. By virtue of (3.7c) the tail of $F_{\text{RT}}(\mathcal{L}, \mathcal{L}')$ at large distances is given by the tail of the resummed multipole-multipole interaction in F^{mm} (3.8) and can be decomposed into a “diffraction” term arising from ϕ^{mm} and a purely quantum contribution described by W defined in (3.9). The corresponding leading tails are

$$\int_0^1 ds \int_0^1 ds' \sum_{q=1}^{+\infty} \sum_{q'=1}^{+\infty} \frac{1}{q!} \frac{1}{q'!} [\lambda_\alpha \xi_x(s)]^q [\lambda_{\alpha'} \xi'_{x'}(s')]^{q'} \frac{\partial^{q+q'} g^{cc}(x, x')}{\partial x^q \partial x'^{q'}} \times \frac{1}{|\mathbf{y}|^3} \quad (3.16)$$

and

$$-\beta e_\alpha e_{\alpha'} \int_0^1 ds \int_0^1 ds' [\delta(s - s') - 1] \lambda_\alpha \xi_x(s) \lambda_{\alpha'} \xi'_{x'}(s') \frac{\partial^2 v(\mathbf{r} - \mathbf{r}')}{\partial x \partial x'} \quad (3.17)$$

The tail (3.16) is integrable for the same reason as the tail (3.15) of F^{mc} . When $|\mathbf{y}|$ goes to infinity while the values of x and x' are kept fixed, the function (3.17) decays as $|\mathbf{y}|^3$ times a function which, after integration over the Brownian measures $\mathcal{D}_{x,\alpha}(\boldsymbol{\xi})$ and $\mathcal{D}_{x',\gamma}(\boldsymbol{\xi}')$, depends on x and x' and converges gaussianly fast to zero over the scale λ_α and $\lambda_{\alpha'}$ respectively. Eventually, thanks to resummations, every diagram in (3.10) is well defined in the thermodynamical limit, and we will consider this limit from now on.

4 Screened potential

4.1 Debye equation for an inhomogeneous fluid

The screened potential ϕ which is defined as the sum of chains (3.6) is the solution of the integral equation

$$\phi(\mathbf{r}, \mathbf{r}') = v(\mathbf{r}, \mathbf{r}') - \frac{1}{4\pi} \int d\mathbf{r}'' \bar{\kappa}^2(x'') v(\mathbf{r}, \mathbf{r}'') \phi(\mathbf{r}'', \mathbf{r}'). \quad (4.1)$$

In (4.1) the positive function $\bar{\kappa}^2(x)$ reads

$$\begin{aligned} \bar{\kappa}^2(x) &\equiv 4\pi\beta \sum_{\alpha} e_{\alpha}^2 \int \mathcal{D}_{x,\alpha}(\xi) z(\mathcal{L}) \\ &= \theta(x) 4\pi\beta \sum_{\alpha} e_{\alpha}^2 z_{\alpha} \left[1 - e^{-2x^2/\lambda_{\alpha}^2} \right], \end{aligned} \quad (4.2)$$

where the second equality arises from (2.14)–(2.16). Far away from the wall $\bar{\kappa}^2(x)$ tends towards its bulk value

$$\kappa^2 \equiv 4\pi\beta \sum_{\alpha} e_{\alpha}^2 z_{\alpha}. \quad (4.3)$$

By using Poisson equation satisfied by Coulomb potential v ,

$$\Delta_{\mathbf{r}} v(\mathbf{r}, \mathbf{r}') = -4\pi\delta(\mathbf{r} - \mathbf{r}'), \quad (4.4)$$

the integral equation (4.1) is shown to be equivalent to a set of partial derivative equations, the explicit expressions of which depend on the signs of x and x' . For $x' > 0$, $\phi(\mathbf{r}, \mathbf{r}')$ is a solution of

$$\Delta_{\mathbf{r}} \phi(\mathbf{r}, \mathbf{r}') - \bar{\kappa}^2(x) \phi(\mathbf{r}, \mathbf{r}') = -4\pi\delta(\mathbf{r} - \mathbf{r}') \quad \text{for } x > 0 \quad (4.5a)$$

and

$$\Delta_{\mathbf{r}} \phi(\mathbf{r}, \mathbf{r}') = 0 \quad \text{for } x < 0. \quad (4.5b)$$

Moreover, the diagrammatic definition (3.6) of ϕ implies that ϕ obeys the same boundary conditions as the electrostatic potential $v(\mathbf{r}, \mathbf{r}')$,

$$\phi(\mathbf{r}, \mathbf{r}') \quad \text{and} \quad \left. \frac{\partial \phi(\mathbf{r}, \mathbf{r}')}{\partial x} \right|_{x \neq x'} \quad \text{are continuous at } x = 0 \quad (4.6a)$$

$$\lim_{|\mathbf{r}| \rightarrow \infty} \phi(\mathbf{r}, \mathbf{r}') = 0. \quad (4.6b)$$

The invariance of the system in directions parallel to the interface implies that the Fourier transform of ϕ along these directions obeys a one-dimensional differential equation with respect to x . We introduce the dimensionless coordinates $\tilde{x} \equiv \kappa x$, $\tilde{\mathbf{y}} \equiv \kappa \mathbf{y}$ and $\tilde{\mathbf{r}} \equiv \kappa \mathbf{r}$ and the dimensionless

screened potential $\tilde{\phi}$ defined by

$$\tilde{\phi}(\tilde{x}, \tilde{x}', \tilde{\mathbf{y}}) = \frac{1}{\kappa} \phi(x, x', \mathbf{y}). \quad (4.7)$$

The dimensionless Fourier transform of $\tilde{\phi}$ along directions parallel to the wall reads

$$\tilde{\phi}(\tilde{x}, \tilde{x}', \mathbf{q}) = \int d\tilde{\mathbf{y}} e^{-i\mathbf{q}\cdot\tilde{\mathbf{y}}} \tilde{\phi}(\tilde{x}, \tilde{x}', \tilde{\mathbf{y}}). \quad (4.8)$$

For $\tilde{x}' > 0$ it is a solution of the differential equations

$$\left\{ \frac{\partial^2}{\partial \tilde{x}^2} - (1 + \mathbf{q}^2) - U(\tilde{x}) \right\} \tilde{\phi}(\tilde{x}, \tilde{x}', \mathbf{q}) = -4\pi\delta(\tilde{x} - \tilde{x}') \quad \text{for } \tilde{x} > 0 \quad (4.9a)$$

and

$$\left\{ \frac{\partial^2}{\partial \tilde{x}^2} - \mathbf{q}^2 \right\} \tilde{\phi}(\tilde{x}, \tilde{x}', \mathbf{q}) = 0 \quad \text{for } \tilde{x} < 0, \quad (4.9b)$$

with the potential function

$$U(\tilde{x}) \equiv -\frac{\sum_{\alpha} e_{\alpha}^2 z_{\alpha} e^{-2\tilde{x}^2/(\kappa\lambda_{\alpha})^2}}{\sum_{\gamma} e_{\gamma}^2 z_{\gamma}}. \quad (4.10)$$

4.2 Series representation of the exact screened potential

It is well known (see e.g. Ref. [13]) that the solution of the one-dimensional differential equation (4.9a) can be formally written in terms of the solutions h of the associated “homogeneous” equation (where the Dirac distribution on the r.h.s. is replaced by zero and) which is valid for $-\infty < \tilde{x} < +\infty$,

$$\left\{ \frac{\partial^2}{\partial \tilde{x}^2} - (1 + \mathbf{q}^2) - U(\tilde{x}) \right\} h(\tilde{x}; \mathbf{q}^2) = 0. \quad (4.11)$$

More precisely, a solution $\tilde{\phi}$ of (4.9a) can be decomposed into the following sum: a linear combination of two independent solutions h^+ and h^- plus a particular solution $\tilde{\phi}_{\text{sing}}$ which is singular when $x = x'$ and is calculated in terms of h^+ and h^- by the so-called Wronskian method. In the following, h^+ (h^-) is chosen to be a solution which vanishes (diverges) when \tilde{x} tends to $+\infty$. Then $\tilde{\phi}_{\text{sing}}$ reads

$$\tilde{\phi}_{\text{sing}}(\tilde{x}, \tilde{x}', \mathbf{q}^2) = -\frac{4\pi}{W(\mathbf{q}^2)} h^-(\inf(\tilde{x}, \tilde{x}'); \mathbf{q}^2) h^+(\sup(\tilde{x}, \tilde{x}'); \mathbf{q}^2), \quad (4.12)$$

where the Wronskian $W(\mathbf{q}^2) \equiv h^-(dh^+/d\tilde{x}) - h^+(dh^-/d\tilde{x})$ is independent of \tilde{x} . Since the differential operator in (4.9a) is self-adjoint, the real potential $\tilde{\phi}$ has the symmetry $\tilde{\phi}(\tilde{x}, \tilde{x}', \mathbf{q}) = \tilde{\phi}(\tilde{x}', \tilde{x}, \mathbf{q})$ when $\tilde{x} > 0$ and $\tilde{x}' > 0$. Then the boundary condition (4.6b) obeyed by $\tilde{\phi}$ enforces that

$$\tilde{\phi}(\tilde{x}, \tilde{x}', \mathbf{q}) = \tilde{\phi}_{\text{sing}}(\tilde{x}, \tilde{x}', \mathbf{q}^2) + Z(|\mathbf{q}|) h^+(\tilde{x}; \mathbf{q}^2) h^+(\tilde{x}'; \mathbf{q}^2), \quad (4.13)$$

where $Z(|\mathbf{q}|)$ is determined by the continuity relations (4.6a).

The particular solution h^+ (h^-) of the “homogeneous” equation (4.11) can be written as the solution $\exp[-\tilde{x}\sqrt{1+\mathbf{q}^2}]$ ($\exp[\tilde{x}\sqrt{1+\mathbf{q}^2}]$) of (4.11) when $U = 0$, times $1 + H^+$ ($1 + H^-$) where the function H^+ (H^-), which describes boundary effects, is chosen to vanish at $\tilde{x} = 0$,

$$h^\pm(\tilde{x}; \mathbf{q}^2) = e^{\mp\tilde{x}\sqrt{1+\mathbf{q}^2}} [1 + H^\pm(\tilde{x}, \mathbf{q}^2)]. \quad (4.14)$$

Then

$$\begin{aligned} \tilde{\phi}_{\text{sing}}(\tilde{x}, \tilde{x}', \mathbf{q}^2) &= -\frac{4\pi}{W(\mathbf{q}^2)} e^{-|\tilde{x}-\tilde{x}'|\sqrt{1+\mathbf{q}^2}} \\ &\times [1 + H^-(\inf(\tilde{x}, \tilde{x}'); \mathbf{q}^2)][1 + H^+(\sup(\tilde{x}, \tilde{x}'); \mathbf{q}^2)]. \end{aligned} \quad (4.15)$$

The Wronskian $W(\mathbf{q}^2)$ proves to take the simple form

$$W(\mathbf{q}^2) = -2\sqrt{1+\mathbf{q}^2} + \left. \frac{\partial H^+(\tilde{x}; \mathbf{q}^2)}{\partial \tilde{x}} \right|_{\tilde{x}=0}. \quad (4.16)$$

Indeed, $H^+(\tilde{x}; \mathbf{q}^2)$ and $H^-(\tilde{x}; \mathbf{q}^2)$ vanish at $\tilde{x} = 0$, and so does $\partial H^-/\partial \tilde{x}$, as can be checked on the formal solution given in next paragraph.

As shown in Ref.[5], H^+ can be written as the formal alternative series

$$H^+(\tilde{x}; \mathbf{q}^2) = -\mathcal{T}^+[1](\tilde{x}; \mathbf{q}^2) + \mathcal{T}^+ [\mathcal{T}^+[1]] (\tilde{x}; \mathbf{q}^2) - \dots \quad (4.17)$$

where the operator \mathcal{T}^+ acting on a function f reads

$$\mathcal{T}^+[f](\tilde{x}; \mathbf{q}^2) \equiv \int_0^{\tilde{x}} dv e^{2v\sqrt{1+\mathbf{q}^2}} \int_v^{+\infty} dt e^{-2t\sqrt{1+\mathbf{q}^2}} U(t) f(t). \quad (4.18)$$

The solution H^- can be similarly written in terms of another formal series

$$H^-(\tilde{x}; \mathbf{q}^2) = \mathcal{T}^-[1](\tilde{x}; \mathbf{q}^2) + \mathcal{T}^- [\mathcal{T}^-[1]] (\tilde{x}; \mathbf{q}^2) + \dots \quad (4.19)$$

with

$$\mathcal{T}^-[f](\tilde{x}; \mathbf{q}^2) \equiv \int_0^{\tilde{x}} dv e^{-2v\sqrt{1+\mathbf{q}^2}} \int_0^v dt e^{2t\sqrt{1+\mathbf{q}^2}} U(t) f(t). \quad (4.20)$$

By combining (4.13)–(4.20), we get a representation of the screened potential $\tilde{\phi}$ in terms of formal series.

These series are bounded by geometric series of $\kappa\lambda$ (with $\lambda = \sup_{\alpha}\{\lambda_{\alpha}\}$), because the Gaussian function U is integrable for all x 's. More precisely, a straightforward calculation shows that

$$\begin{aligned} \mathcal{T}^+[1](\tilde{x}) = & -\frac{\sqrt{\pi}}{4\sqrt{2}\sqrt{1+\mathbf{q}^2}} \frac{\sum_{\alpha} e_{\alpha}^2 z_{\alpha} \tilde{\lambda}_{\alpha}}{\sum_{\gamma} e_{\gamma}^2 z_{\gamma}} \left\{ \text{Erf} \left(\frac{\sqrt{2}\tilde{x}}{\tilde{\lambda}_{\alpha}} \right) \right. \\ & + e^{(\tilde{\lambda}_{\alpha}\sqrt{1+\mathbf{q}^2})^2/2} \left[e^{2\tilde{x}\sqrt{1+\mathbf{q}^2}} \text{Erfc} \left(\frac{\sqrt{2}\tilde{x}}{\tilde{\lambda}_{\alpha}} + \frac{\tilde{\lambda}_{\alpha}\sqrt{1+\mathbf{q}^2}}{\sqrt{2}} \right) \right. \\ & \left. \left. - \text{Erfc} \left(\frac{\tilde{\lambda}_{\alpha}\sqrt{1+\mathbf{q}^2}}{\sqrt{2}} \right) \right] \right\}, \quad (4.21) \end{aligned}$$

where $\tilde{\lambda}_{\alpha} = \kappa\lambda_{\alpha}$, and this expression obeys the inequality

$$|\mathcal{T}^+[1](\tilde{x})| < \kappa\lambda. \quad (4.22)$$

4.3 $\kappa\lambda$ -expansion of the screened potential

In Section 5 we will restrict our explicit calculations to a low-degeneracy and weak-coupling regime (see (1.4) and (1.7)). In this regime $\kappa\lambda$ is also negligible with respect to 1 : the de Broglie thermal wavelengths λ_{α} 's are small compared with the typical screening length κ^{-1} .

Let $\tilde{\phi}^{(0)}$ be the solution of equation (4.9a) when the profile $\bar{\kappa}^2(x)$ is replaced by its bulk limit κ^2 . The above formal series for H^+ and H^- provide a systematic expansion of $\tilde{\phi} - \tilde{\phi}^{(0)}$ in terms of the ratios of the length scales λ_{α} 's, over which $\bar{\kappa}^2(x)$ varies, and the length scale κ^{-1} , which is the limit of $\bar{\kappa}^{-1}(x)$ when x goes to infinity. The expansions of H^+ and H^- are absolutely and uniformly convergent with respect to the variable x for values of $\kappa\lambda$ smaller than some finite value, because they are bounded by geometric series. As a result,

$$\tilde{\phi}(\tilde{x}, \tilde{x}', \tilde{\mathbf{y}}) = \tilde{\phi}^{(0)}(\tilde{x}, \tilde{x}', \tilde{\mathbf{y}}) + \mathcal{O}(\kappa\lambda), \quad (4.23)$$

where the leading-order term $\tilde{\phi}^{(0)}$ is equal to $\kappa^{-1}\phi^{(0)}(\mathbf{r}, \mathbf{r}')$ (see (4.7)). By definition, $\phi^{(0)}(\mathbf{r}, \mathbf{r}')$ is the solution of

$$\Delta_{\mathbf{r}}\phi^{(0)}(\mathbf{r}, \mathbf{r}') - \theta(x)\kappa^2\phi^{(0)}(\mathbf{r}, \mathbf{r}') = -4\pi\delta(\mathbf{r} - \mathbf{r}'), \quad (4.24)$$

with the same boundary conditions as $\phi(\mathbf{r}, \mathbf{r}')$. According to (4.13), we get

$$\tilde{\phi}^{(0)}(\tilde{x}, \tilde{x}', \mathbf{q}) = \frac{2\pi}{\sqrt{1+\mathbf{q}^2}} \left\{ e^{-|\tilde{x}-\tilde{x}'|\sqrt{1+\mathbf{q}^2}} + \frac{\sqrt{1+\mathbf{q}^2}-q}{\sqrt{1+\mathbf{q}^2}+q} e^{-(\tilde{x}+\tilde{x}')\sqrt{1+\mathbf{q}^2}} \right\}. \quad (4.25)$$

Moreover, by definition of the screened potential, the correction $\mathcal{O}(\kappa\lambda)$ in (4.23) is independent of the root-point species α and α' . As shown in Section 5.3, the latter property implies that the contribution to density profiles from this $\mathcal{O}(\kappa\lambda)$ -correction in $\tilde{\phi}$ is canceled at first order in $\kappa\lambda$ by the neutrality constraint (2.11) on fugacities. It is the reason why we do not write the explicit expression of the term $\mathcal{O}(\kappa\lambda)$ in (4.23).

5 Weak-coupling expansions

5.1 Subregime for parameters ε and $(\lambda/a)^3$

In the weak-coupling and low-degeneracy regime (1.7) and (1.4), only a finite number of resummed Mayer diagrams in the representation (3.10) of the loop-density $\rho(\mathcal{L})$ contribute at lowest orders in the classical coupling parameter $\varepsilon \equiv (1/2)\kappa\beta e^2$. Moreover diagram contributions may be also expanded in powers of $\kappa\lambda$.

Indeed, $\kappa\lambda$ is a function of the two independent parameters $(\lambda/a)^3$ and ε : by virtue of (1.6),

$$\kappa\lambda \propto \frac{\lambda}{a} \varepsilon^{1/3}, \quad (5.1)$$

and $\kappa\lambda \ll 1$ in the considered regime (1.7) and (1.4). Then the screened potential ϕ , which is involved both in screened fugacities and in resummed bonds, can be expanded in powers of $\kappa\lambda$, as well as the functions resulting from integrations over Brownian paths. As shown by the scaling analysis performed in next Sections 5.2 and 5.3, the diagrammatic representation of the particle density derived from (2.26) and (3.10) provides a systematic expansion of $\rho_\alpha(x)$ in powers of parameters ε and $\kappa\lambda$, where exchange effects are neglected.

More precisely, we will show that, because of quantum dynamics, the first coupling corrections to the ideal-gas particle density is a sum of two terms of order ε and $\kappa\lambda$ respectively, and the next contributions are of order

$$\varepsilon^2, \varepsilon^2 |\ln(\kappa\lambda)|, \varepsilon \cdot \kappa\lambda, (\kappa\lambda)^2, \left(\frac{\lambda}{a}\right)^3 Q_w \left(-\frac{\beta e^2}{\lambda}\right), \quad (5.2)$$

with

$$\left(\frac{\lambda}{a}\right)^3 \propto \frac{(\kappa\lambda)^3}{\varepsilon} \quad \text{and} \quad \frac{\beta e^2}{\lambda} \propto \frac{\varepsilon}{\kappa\lambda} \quad (5.3)$$

$Q_w(t)$ is expected to vanish at $t = 0$ by analogy with the bulk function Q defined in Ref.[14]. On the other hand, exchange corrections, which have been neglected from the start, are of order

$$\left(\frac{\lambda}{a}\right)^3 E_w\left(-\frac{\beta e^2}{\lambda}\right) \quad (5.4)$$

where $E_w(t)$ is expected to vanish as t goes to zero, for the same reason as $Q_w(t)$.

As a consequence, we shall be allowed to retain only the corrections linear in ε and $\kappa\lambda$ in $\rho_\alpha(x)$, if these terms are larger than the exchange corrections of order (5.4) and the coupling corrections of order (5.3). We consider the subregime where

$$\varepsilon^2 \leq \left(\frac{\lambda}{a}\right)^3 \ll \varepsilon, \quad (5.5)$$

In (5.5) $\varepsilon^2 \leq (\lambda/a)^3$ means that the ratio of ε^2 and $(\lambda/a)^3$ is either kept fixed or tends to zero when both ε and λ/a vanish. In other words, $\beta e^2/\lambda$ is kept fixed – i.e. the temperature remains fixed – or vanishes – i.e. the temperature goes to infinity. In this subregime the condition

$$\left(\frac{\lambda}{a}\right)^3 F\left(-\frac{\beta e^2}{\lambda}\right) \ll \varepsilon, \quad (5.6)$$

with $F = Q_w$ or E_w , is met, as well as the condition

$$\left(\frac{\lambda}{a}\right)^3 F(-\beta e^2/\lambda) \ll \kappa\lambda. \quad (5.7)$$

Similarly, inequalities $\varepsilon^2 \ll \kappa\lambda$, $\varepsilon^2 |\ln(\kappa\lambda)| \ll \varepsilon$, $\varepsilon^2 |\ln(\kappa\lambda)| \ll \kappa\lambda$, and $(\kappa\lambda)^2 \ll \varepsilon$, are also satisfied. Eventually, in the subregime (5.5), which can be rewritten as $\varepsilon^3 \leq (\kappa\lambda)^3 \ll \varepsilon^2$ by virtue of (5.1), we may retain only contributions of order ε and $\kappa\lambda$, and the neglected terms are of order $\mathcal{O}(\eta^2)$, where η^2 is a generic notation for the terms in (5.2) and (5.4),

$$\mathcal{O}(\eta^2) \equiv \mathcal{O}((5.2), (5.4)). \quad (5.8)$$

5.2 Screened loop fugacity

In this section we calculate the $\kappa\lambda$ -expansion of the screened fugacities (3.11). As shown in Ref. [1], the free energy $e_\alpha^2 \mathcal{V}_{\text{cloud}}^{\text{sc}}$ is associated with the “geometric” repulsion from the wall due to the deformation of the screening cloud surrounding every charge near a boundary. According to (3.12) and

the fact that $(\phi - v)$ and its derivative are continuous (because ϕ and v have the same singularity when $\mathbf{r} = \mathbf{r}'$),

$$\mathcal{V}_{\text{cloud}}^{\text{sc}}(\mathcal{L}) = V_{\text{cloud}}^{\text{sc}}(\mathbf{r}) + \frac{1}{\kappa} \mathcal{O}(\kappa\lambda). \quad (5.9)$$

(5.9) is the Taylor expansion of $\mathcal{V}_{\text{cloud}}^{\text{sc}}$ around its classical value

$$V_{\text{cloud}}^{\text{sc}}(\mathbf{r}) \equiv \frac{1}{2} [\phi - v](\mathbf{r}, \mathbf{r}). \quad (5.10)$$

(We stress that $V_{\text{cloud}}^{\text{sc}}(\mathbf{r})$ has no singularity in the range $0 \leq x$ so that no classical spurious singularity is introduced by the expansion (5.9).) The $\kappa\lambda$ -expansion (4.23) of the screened potential $\tilde{\phi}$ leads to

$$V_{\text{cloud}}^{\text{sc}}(\mathbf{r}) = V_{\text{cloud}}^{\text{sc}(0)}(\mathbf{r}) + \frac{1}{\kappa} \mathcal{O}(\kappa\lambda), \quad (5.11)$$

where at first order

$$-\beta e_{\alpha}^2 V_{\text{cloud}}^{\text{sc}(0)}(\mathbf{r}) = -\frac{\beta e_{\alpha}^2}{2} [\phi^{(0)} - v](\mathbf{r}, \mathbf{r}) = \varepsilon_{\alpha} [1 - \overline{L}(\kappa x)]. \quad (5.12)$$

In (5.12) we have used the definition

$$\varepsilon_{\alpha} \equiv \frac{1}{2} \kappa \beta e_{\alpha}^2. \quad (5.13)$$

By virtue of (4.25),

$$\begin{aligned} \overline{L}(u) &\equiv \int_1^{\infty} dt \frac{e^{-2tu}}{(t + \sqrt{t^2 - 1})^2} \\ &= e^{-2u} \left[\frac{1}{2u} + \frac{1}{u^2} + \frac{1}{2u^3} \right] - \frac{1}{u} K_2(2u), \end{aligned} \quad (5.14)$$

where $K_2(2u)$ is a Bessel function, which decays proportionally to $\exp(-2u)/\sqrt{u}$ at large u . $\overline{L}(u)$ is a continuous positive decreasing function for $u \geq 0$. Therefore $\overline{L}(u)$ is bounded by $\overline{L}(0) = 1/3$ and, since ε_{α} is small, we can expand the exponential function in the definition (3.11) of screened loop fugacities. We get

$$z^{\text{sc}}(\mathcal{L}) = \theta(x) z_{\alpha} \left\{ 1 + \varepsilon_{\alpha} [1 - \overline{L}(\kappa x)] + \mathcal{O}(\varepsilon \cdot \kappa\lambda) \right\}. \quad (5.15)$$

Since $\overline{L}(u)$ vanishes exponentially fast when u goes to infinity, $z^{\text{sc}}(\mathcal{L})$ tends to $z_{\alpha} \{1 + \varepsilon_{\alpha}\}$ far away from the wall.

5.3 Diagram contributions at leading orders

5.3.1 Bond F^{cc}

The integral associated with the diagram with one F^{cc} -bond reads

$$\int d\mathcal{L}' z^{\text{sc}}(\mathcal{L}') F^{\text{cc}}(\mathcal{L}, \mathcal{L}') = -\beta e_\alpha \sum_\gamma e_\gamma \int d\mathbf{r}' \phi(\mathbf{r}, \mathbf{r}') \bar{z}_\gamma^{\text{sc}}(x'), \quad (5.16)$$

where the screened fugacity $\bar{z}_\alpha^{\text{sc}}(x)$ is defined as

$$\bar{z}_\alpha^{\text{sc}}(x) \equiv \int \mathcal{D}_{x,\alpha}(\xi) z^{\text{sc}}(\mathcal{L}). \quad (5.17)$$

By using the value (5.15) of the screened loop fugacity and the integral (2.16) of the path measure, we get

$$\bar{z}_\alpha^{\text{sc}}(x) = z_\alpha \left[1 - e^{-2x^2/\lambda_\alpha^2} \right] \left\{ 1 + \varepsilon_\alpha [1 - \bar{L}(\kappa x)] \right\} + z_\alpha \mathcal{O}(\varepsilon, \kappa \lambda). \quad (5.18)$$

By virtue of (4.23), the leading-order terms in (5.16) arise from the structure

$$-\beta e_\alpha \sum_\gamma e_\gamma z_\gamma \int_{x'>0} d\mathbf{r}' \left[\phi^{(0)}(\mathbf{r}, \mathbf{r}') + \mathcal{O}(\kappa \lambda) \right] \left[1 - e^{-2x'^2/\lambda_\gamma^2} \right] \left[1 + \mathcal{O}_\gamma(\varepsilon) \right], \quad (5.19)$$

where $\mathcal{O}_\gamma(\varepsilon)$ is a term of order ε which depends on the species γ . ($\mathcal{O}_\gamma(\varepsilon)$ is the screened self-energy term in $\bar{z}_\gamma^{\text{sc}}(x)$.)

The *a priori* leading-order term in (5.19) is obtained by retaining only the two constants 1 in brackets and $\phi^{(0)}(\mathbf{r}, \mathbf{r}')$. This term is independent of the de Broglie wavelengths, because $\phi^{(0)}(\mathbf{r}, \mathbf{r}')$ is purely classical and involves only the length scale $1/\kappa_D$. By virtue of (4.25),

$$\int_{x'>0} d\mathbf{r}' \phi^{(0)}(\mathbf{r}, \mathbf{r}') = \frac{2\pi}{\kappa^2} \int_0^{+\infty} d\tilde{x}' \left\{ e^{-|\tilde{x}-\tilde{x}'|} + e^{-(\tilde{x}+\tilde{x}')} \right\}. \quad (5.20)$$

As a consequence, the leading term in (5.19) is both $\mathcal{O}(\varepsilon^0)$ and $\mathcal{O}((\kappa \lambda)^0)$, namely, before summation over γ ,

$$\int d\mathbf{r}' \int \mathcal{D}_{x',\gamma}(\xi') z^{\text{sc}}(\mathcal{L}') F^{\text{cc}}(\mathcal{L}, \mathcal{L}') = \mathcal{O}(1). \quad (5.21)$$

However, after summation over species, the $\mathcal{O}(1)$ contribution in (5.16), where the quantity $\sum_\gamma e_\gamma z_\gamma$ is factorized, is exactly equal to zero because of the neutrality condition (2.11) imposed on fugacities. Moreover, without condition (2.11), we would have to consider an infinite number of

diagrams at leading order, because the addition of a “star” subdiagram $\prod_{i=2}^n [\int d\mathcal{L}_i z^{\text{sc}}(\mathcal{L}_i) F^{\text{cc}}(\mathcal{L}', \mathcal{L}_i)]$, with an arbitrary number n , to the diagram $\int d\mathcal{L}' z^{\text{sc}}(\mathcal{L}') F^{\text{cc}}(\mathcal{L}, \mathcal{L}')$ would also yield a contribution of leading order $\mathcal{O}(1)$. Nevertheless, we notice that, after summation over all diagrams, the final expansion of the density must be independent of whether the condition on fugacities is fulfilled or not, because of the degeneracy among fugacities discussed in Section 2.2.

In fact, the diagram with one bond F^{cc} contributes at orders ε and $\kappa\lambda$,

$$\int d\mathcal{L}' z^{\text{sc}}(\mathcal{L}') F^{\text{cc}}(\mathcal{L}, \mathcal{L}') = \mathcal{O}(\varepsilon, \kappa\lambda) \quad (5.22)$$

The contribution of order $\mathcal{O}(\varepsilon)$ comes from $\phi^{(0)}(\mathbf{r}, \mathbf{r}') \times \mathcal{O}_\gamma(\varepsilon)$ in (5.19), and it has been calculated in Ref. [5]. The contribution of order $\kappa\lambda$ arising from the product of constants 1 in (5.19) times the term of order $\kappa\lambda$ in the expansion of $\phi(\mathbf{r}, \mathbf{r}')$ is canceled by the neutrality condition (2.11). (This is also true for the whole $\kappa\lambda$ -expansion of $\phi(\mathbf{r}, \mathbf{r}')$, because all terms which depend on a species γ only through the product $e_\gamma z_\gamma$ are canceled when the summation over γ is performed.) Therefore, the contribution of order $\kappa\lambda$ arises only from $\phi^{(0)}(\mathbf{r}, \mathbf{r}') \exp[-2x'^2/\lambda_\gamma^2]$ in (5.19). The factor $\kappa\lambda$ is yielded by the x' -integration of the Gaussian term which arises from the integrated quantum measure (2.16). Indeed, for any bounded and integrable function f which decays less quickly than $\exp[-2x^2/\lambda_\alpha^2]$ at large x

$$\begin{aligned} \int_0^{+\infty} \kappa dx e^{-2x^2/\lambda_\alpha^2} f(\kappa x) &\underset{\kappa\lambda_\alpha \rightarrow 0}{\sim} \kappa\lambda_\alpha \times f(0) \int_0^{+\infty} dt e^{-2t^2} \\ &= \mathcal{O}(\kappa\lambda_\alpha) \times \mathcal{O}\left(\int_0^{+\infty} du f(u)\right). \end{aligned} \quad (5.23)$$

(The Gaussian factor in the integral on the l.h.s. of (5.23) makes this integral convergent over the scale λ_γ , and not κ^{-1} as it would be the case if this factor were not here.) As shown in Appendix B, the same mechanism also operates for the x' -integration of odd moments of a Brownian path ξ' (involved in diagrams with F^{cm} -bonds), because these moments decay gaussianly fast to zero at large x' over the scales λ_α 's (see for instance (2.18)), contrary to even moments which tend to their non-zero bulk values away from the wall.

5.3.2 Other resummed bonds

As shown in Appendix B, by combining previous arguments, Taylor expansions around classical expressions and construction rule (3.13) about fugacities, where $z^{\text{sc}}(\mathcal{L}') - z(\mathcal{L}') = z_\alpha \mathcal{O}(\varepsilon)$, a simple scaling analysis shows that diagrams with one bond, F^{cm} , F^{mc} , $[F^{\text{cc}}]^2/2$, $F^{\text{cc}}F^{\text{cm}}$, $[F^{\text{cm}}]^2/2$,

$F^{cc}F^{mc}$, or $[F^{mc}]^2/2$ are of orders equal to either $(\kappa\lambda)^2$, $\varepsilon \cdot \kappa\lambda$, ε^2 , $\varepsilon(\kappa\lambda)^2$, $\varepsilon^2 \cdot \kappa\lambda$, or $\varepsilon^2 \cdot (\kappa\lambda)^2$. The order of the contribution from the bond F_{RT} is determined by analogy with its order in the bulk case.

5.3.3 Global results

As a result, the complete scaling analysis shows that, at first order in ε and $\kappa\lambda$, the loop density comes from (3.10) where only one diagram, namely the diagram with a single F^{cc} -bond, is retained in the argument of the exponential. Moreover, the expression of this first-order contribution involves only the lowest-order term $\phi^{(0)}(\mathbf{r}, \mathbf{r}')$ in the $\kappa\lambda$ -expansion (4.23) of the screened potential. The loop density reads

$$\begin{aligned} \rho(\mathcal{L}) = z^{\text{sc}}(\mathcal{L}) \\ \times \exp \left\{ -\beta e_\alpha \sum_\gamma e_\gamma \int d\mathbf{r}' \phi^{(0)}(\mathbf{r}, \mathbf{r}') \left(\int \mathcal{D}_{x', \gamma}(\boldsymbol{\xi}') z^{\text{sc}}(\mathcal{L}') \right) \right. \\ \left. + \mathcal{O}((5.2)) \right\}. \quad (5.24) \end{aligned}$$

$$\rho(\mathcal{L}) = z^{\text{sc}}(\mathcal{L}) \exp \left\{ \mathcal{L} \text{---} \overset{F^{cc}}{\bullet} z^{\text{sc}}(\mathcal{L}') + \mathcal{O}(\eta^2) \right\}$$

Figure 6: Diagrammatic expression of the loop density at first order in ε and $\kappa\lambda$.

Since the argument of the exponential in (5.24) proves to be a bounded function of order ε and $\kappa\lambda$, the loop density is given at first order in ε and $\kappa\lambda$ by linearizing the exponential in (5.24). According to (2.26), the particle density profile is obtained by performing the path integration $\int \mathcal{D}_{x, \gamma}(\boldsymbol{\xi})$ with the result

$$\rho_\alpha(x) = \bar{z}_\alpha^{\text{sc}}(x) \left\{ 1 - \beta e_\alpha \sum_\gamma e_\gamma \int d\mathbf{r}' \bar{z}_\gamma^{\text{sc}}(x') \phi^{(0)}(\mathbf{r}, \mathbf{r}') + \mathcal{O}(\eta^2) \right\}, \quad (5.25)$$

where $\bar{z}_\alpha^{\text{sc}}(x)$ is given in (5.18) and η^2 is defined in (5.8).

5.4 Electrostatic potential

In this section we show how the integral involved in the expression (5.25) is related to the potential $\Phi(x)$, which is defined as the difference between the

electrostatic potential created by the fluid and the electrostatic potential V_R in the particle reservoir (located in the bulk). This potential obeys Poisson equation

$$\frac{d^2\Phi}{dx^2}(x) = -4\pi \sum_{\alpha} e_{\alpha} \rho_{\alpha}(x) \quad (5.26)$$

with the boundary conditions : Φ and $d\Phi/dx$ tend to 0 when x goes to $+\infty$. The condition about the derivative of Φ arises from the absence of any net electrostatic field in the bulk for a Coulomb fluid at equilibrium. The condition about Φ fixes the electrostatic potential reference. The definition of $\Phi(x)$ leads to the integral representation

$$\Phi(x) = -4\pi \int_x^{+\infty} dx' (x' - x) \sum_{\alpha} e_{\alpha} \rho_{\alpha}(x'). \quad (5.27)$$

As in the classical case [5], the structure (5.25) of density profiles can be rewritten in the form

$$\rho_{\alpha}(x) = \bar{z}_{\alpha}^{\text{sc}}(x) \left[1 - \beta e_{\alpha} G(x) \right] \quad (5.28)$$

with

$$G(x) \equiv \sum_{\gamma} e_{\gamma} \int d\mathbf{r}' \bar{z}_{\gamma}^{\text{sc}}(x') \phi^{(0)}(\mathbf{r}, \mathbf{r}'). \quad (5.29)$$

As checked in Section 5.5, at leading order $G(x)$ is a function of κx . Therefore, according to (5.18) and (5.23), the contribution from $-\beta \sum_{\alpha} e_{\alpha}^2 [\bar{z}_{\alpha}^{\text{sc}}(x) - z_{\alpha}] G(x)$ to the integral in (5.27) is a correction of relative orders $\mathcal{O}(\kappa\lambda)$ and $\mathcal{O}(\varepsilon)$ with respect to the leading contribution from

$$\sum_{\alpha} e_{\alpha} \bar{z}_{\alpha}^{\text{sc}}(x) - \beta \left(\sum_{\alpha} e_{\alpha}^2 z_{\alpha} \right) G(x). \quad (5.30)$$

Therefore, the argument of Section 5.4 in Ref. [5] holds. It reads as follows. According to its definition and the partial derivative equation (4.24) satisfied by $\phi^{(0)}$, $G(x)$ obeys the differential equation

$$\frac{d^2 G(x)}{dx^2} = -4\pi \sum_{\alpha} e_{\alpha} \bar{z}_{\alpha}^{\text{sc}}(x) + \kappa^2 G(x). \quad (5.31)$$

Since $dG(x)/dx$ is finite and decays to zero when x goes to infinity, combination of (5.27), (5.30), and (5.31) implies that the electrostatic potential is merely

$$\Phi(x) = \left[G(x) - \lim_{x \rightarrow +\infty} G(x) \right] + \frac{1}{\beta e} \mathcal{O}(\varepsilon, \kappa\lambda), \quad (5.32)$$

where $\mathcal{O}(\varepsilon, \kappa\lambda)$ denotes a sum of terms of order ε and $\kappa\lambda$ respectively.

Eventually, by virtue of (5.18) and (5.32), the density profile (5.28) can be rewritten in terms of the bulk density and the electrostatic potential drop $\Phi(x)$ created by the fluid as

$$\rho_\alpha(x) = \rho_\alpha^B \left[1 - e^{-2x^2/\lambda_\alpha^2} \right] \left\{ 1 - \varepsilon_\alpha \bar{L}(\kappa x) - \beta e_\alpha \Phi(x) \right\} + \rho_\alpha^B \mathcal{O}(\eta^2), \quad (5.33)$$

where the bulk density is given by

$$\rho_\alpha^B \equiv \lim_{x \rightarrow +\infty} \rho_\alpha(x) = z_\alpha \left\{ 1 + \varepsilon_\alpha - \beta e_\alpha \lim_{x \rightarrow +\infty} G(x) + \mathcal{O}(\eta^2) \right\}. \quad (5.34)$$

Since the bulk density ρ_α^B coincides with z_α at leading order, κ_D defined in (1.5) is also equal to κ at leading order

$$\kappa_D = \kappa \left[1 + \mathcal{O}(\varepsilon) \right] \quad \text{and} \quad \varepsilon_D = \varepsilon \left[1 + \mathcal{O}(\varepsilon) \right]. \quad (5.35)$$

This will enable us to consider the Debye screening length as the reference length scale for classical effects when writing the final results in next section.

5.5 Decomposition into classical and quantum contributions

In the density profile (5.33), the term involving \bar{L} is purely classical, whereas the electrostatic potential can be split into a classical contribution $\Phi^{\text{cl}(\varepsilon)}$ of order $\mathcal{O}(\varepsilon/(\beta e))$ and a quantum contribution $\Phi^{\text{qu}(\kappa\lambda)}$ of order $\mathcal{O}(\kappa\lambda/(\beta e))$,

$$\Phi(x) = \Phi^{\text{qu}(\kappa\lambda)}(x) + \Phi^{\text{cl}(\varepsilon)}(x) + \frac{1}{\beta e} \mathcal{O}(\eta^2). \quad (5.36)$$

According to (5.32), $\Phi^{\text{cl}(\varepsilon)}(x) = G^{\text{cl}(\varepsilon)}(x) - \lim_{x \rightarrow +\infty} G^{\text{cl}(\varepsilon)}(x)$ with, by virtue of (5.29), (5.18), and of the neutrality constraint (2.11) upon fugacities,

$$G^{\text{cl}(\varepsilon)}(x) = \sum_\gamma e_\gamma \int d\mathbf{r}' \theta(x') z_\gamma \varepsilon_\gamma \left[1 - \bar{L}(\kappa x') \right] \phi^{(0)}(\mathbf{r}, \mathbf{r}'), \quad (5.37)$$

whereas $\Phi^{\text{qu}(\kappa\lambda)}$ is the leading term in the expansion of

$$- \sum_\gamma e_\gamma \int d\mathbf{r}' \theta(x') z_\gamma e^{-2x'^2/\lambda_\gamma^2} \phi^{(0)}(\mathbf{r}, \mathbf{r}'). \quad (5.38)$$

Since $\int d\mathbf{y}\phi^{(0)}(x, x', \mathbf{y})$ is a function of $\kappa x'$ which decays exponentially fast when $\kappa x'$ goes to infinity, according to (5.23),

$$\Phi^{\text{qu}(\kappa\lambda)}(x) = \int_0^{+\infty} dx' \left(- \sum_{\gamma} e_{\gamma} z_{\gamma} e^{-2x'^2/\lambda_{\gamma}^2} \right) \int d\mathbf{y}\phi^{(0)}(x, x' = 0, \mathbf{y}). \quad (5.39)$$

The classical part $\Phi^{\text{cl}(\varepsilon)}$ in the electrostatic potential has already been calculated in Ref.[1] with the result

$$\Phi^{\text{cl}(\varepsilon)}(x) = -A \overline{M}(\kappa_D x), \quad (5.40)$$

where the function \overline{M} is

$$\overline{M}(u) = \int_1^{\infty} dt \frac{e^{-2tu} - 2te^{-u}}{1 - (2t)^2} \frac{1}{(t + \sqrt{t^2 - 1})^2}, \quad (5.41)$$

and the constant A reads

$$A = \sqrt{\pi\beta} \frac{\sum_{\gamma} e_{\gamma}^3 \rho_{\gamma}^B}{\sqrt{\sum_{\alpha} e_{\alpha}^2 \rho_{\alpha}^B}}. \quad (5.42)$$

In (5.40), the argument of \overline{M} has been written $\kappa_D x$ in place of κx , by virtue of (5.35).

The purely quantum part of the electrostatic potential drop is derived from (5.39). According to the expression of $\int d\mathbf{y}\phi^{(0)}(x, x', \mathbf{y})$ already used in (5.20),

$$\Phi^{\text{qu}(\kappa\lambda)}(x) = -\hbar \mathcal{B} e^{-\kappa_D x}, \quad (5.43)$$

where the constant \mathcal{B} depends only on the fluid composition

$$\mathcal{B} = \frac{\pi}{\sqrt{2}} \frac{\sum_{\gamma} (e_{\gamma}/\sqrt{m_{\gamma}}) \rho_{\gamma}^B}{\sqrt{\sum_{\alpha} e_{\alpha}^2 \rho_{\alpha}^B}}. \quad (5.44)$$

We notice that the total electrostatic potential drop between the wall and the fluid bulk (set as the reference of electrostatic potentials) is equal at leading order to

$$\Phi(0) = -\frac{A}{2} \left(\ln 3 - 1 - \frac{\pi}{\sqrt{3}} \right) - \hbar \mathcal{B}. \quad (5.45)$$

$\Phi(0)$ includes both classical and quantum corrections.

The structure of quantum particle densities derived from (5.33), (5.40) and (5.43) is summarized in (1.10). In the fugacity expansion of the bulk density ρ_{α}^B , the explicit first-order correction to the value z_{α} in an ideal gas is derived from (5.34) and the explicit value of $G(x)$. Since $G^{\text{qu}(\kappa\lambda)}(x)$

tends towards zero when x goes to infinity, the relation between ρ_α^B and z_α does not include quantum contributions proportional to \hbar and reads

$$\rho_\alpha^B = z_\alpha \left\{ 1 + \beta e_\alpha^2 \sqrt{\pi\beta \sum_\gamma e_\gamma^2 \rho_\gamma^B} - \beta e_\alpha \sqrt{\pi\beta} \frac{\sum_\gamma e_\gamma^3 \rho_\gamma^B}{\sqrt{\sum_\alpha e_\alpha^2 \rho_\alpha^B}} + \mathcal{O}(\eta^2) \right\}. \quad (5.46)$$

Indeed, in the bulk, the spherical symmetry enforces quantum-dynamical coupling effects to be at least of order $(\kappa\lambda)^2$, proportional to \hbar^2 , whereas exchange effects are at least of order $(\lambda/a)^3$, proportional to \hbar^3 . The expression (5.46) is in agreement with the result (5.28) of Ref.[3] calculated directly in the bulk. It does satisfy the electroneutrality condition (1.13).

The expression (1.10) of the quantum density profile at first order in ε and $\kappa\lambda$ can be rewritten in terms of the densities $\rho_\alpha^{\text{cl}(\varepsilon)}$ at first order in ε in the corresponding classical system,

$$\rho_\alpha^{\text{cl}(\varepsilon)}(x) = \rho_\alpha^B \left[1 - \varepsilon_\alpha \bar{L}(\kappa_D x) - \beta e_\alpha \Phi^{\text{cl}(\varepsilon)}(x) \right], \quad (5.47)$$

where \bar{L} is defined in (5.14). At this leading order the classical density profile does not involve the short-range repulsion that must be introduced in order to prevent the collapse of the system in the limit where \hbar tends to zero (see e.g. Ref.[1]). Indeed, (5.47) is obtained in a subregime where the range σ of the short-distance repulsion is such that $\varepsilon^2 \leq (\sigma/a)^3 \ll \varepsilon$. We get

$$\rho_\alpha(x) = \left[1 - e^{-2x^2/\lambda_\alpha^2} \right] \left\{ \rho_\alpha^{\text{cl}(\varepsilon)}(x) - \rho_\alpha^B \beta e_\alpha \Phi^{\text{qu}(\kappa\lambda)}(x) \right\} + \rho_\alpha^B \mathcal{O}(\eta^2). \quad (5.48)$$

The latter expression displays two quantum effects. We stress that the effect linked to the vanishing of wave-functions has an essential singularity in \hbar . The quantum contribution linear in \hbar in the electrostatic potential is allowed by the breakdown of spherical symmetry, whereas bulk quantum effects in the physical regime of interest appear only at order \hbar^2 [3], as already mentioned.

6 Generic properties

6.1 Density profiles

The structure (1.10) of density profiles is ruled by the competition between three effects. The purely quantum contribution $\left[1 - e^{-2x^2/\lambda_\alpha^2} \right]$ arises from the vanishing of wave-functions inside the wall. In the physical regime of interest this effect is the same one as in an ideal gas (see (1.2)), up to

amplitude corrections arising from Coulomb coupling. The second term, involving the function \bar{L} , describes the geometric repulsion due to the deformation of screening clouds near a wall [1]. Indeed, a charge and its surrounding screening cloud are more stable in a spherical geometry than in the dissymmetric configurations enforced by the presence of a wall. This effect is purely classical at the order of the present calculation. The term $e_\alpha \Phi(x)$ describes the interaction between a particle with a charge e_α and the electrostatic potential drop, created by the fluid itself, with respect to the bulk (set as the reference of electrostatic potentials). This contribution contains both quantum and classical effects.

In the very vicinity of the wall, for $x \leq \lambda \ll \xi_D$ (with $\lambda = \sup_\alpha \{\lambda_\alpha\}$), densities are mostly ruled by the quantum effect of the cancellation of wave-functions inside the wall,

$$\rho_\alpha(x) \underset{x \leq \lambda \ll \xi_D}{\sim} \rho_\alpha^B \left[1 - e^{-2x^2/\lambda_\alpha^2} \right] \left\{ 1 - \frac{1}{6} \kappa_D \beta e_\alpha^2 - \beta e_\alpha \Phi(0) \right\}, \quad (6.1)$$

where $\Phi(0)$ is given in (5.45). The heavier a particle species is, the steeper the vanishing of its density occurs, since dynamical quantum effects are less important for heavy particles. Densities and their first derivatives are continuous on the wall, as expected, since densities involve the squared moduli of wavefunctions and the latter ones are continuous at the boundary of a wall with a possible step variation in their first derivatives.

At distances from the wall large compared with the quantum de Broglie wavelengths, $x \gg \lambda$, densities vary over the classical Debye screening length

$$\rho_\alpha(x) \underset{\lambda \ll x \leq \xi_D}{\sim} \rho_\alpha^B \left\{ 1 - \frac{1}{2} \kappa_D \beta e_\alpha^2 \bar{L}(\kappa_D x) + \beta e_\alpha \left[A \bar{M}(\kappa_D x) + \hbar \mathcal{B} e^{-\kappa_D x} \right] \right\}, \quad (6.2)$$

where A and \mathcal{B} are given in (5.42) and (5.44) respectively. In this region, density profiles are determined by the interplay between the effect of the classical geometric repulsion described by $\bar{L}(\kappa_D x)$ and the effect of the electrostatic potential, with both classical and quantum origins. $\bar{L}(\kappa_D x)$ and $\bar{M}(\kappa_D x)$ vanish exponentially fast over the scales $\xi_D/2$ and ξ_D respectively.

As a consequence, at distances from the wall large compared with the classical Debye screening length ξ_D , the contribution from the electrostatic potential dominates in the density profiles

$$\frac{\rho_\alpha(x) - \rho_\alpha^B}{\rho_\alpha^B} \underset{x \gg \xi_D}{\sim} -\beta e_\alpha \Phi_{\text{as}} e^{-\kappa_D x}, \quad (6.3)$$

where

$$\Phi_{\text{as}} = -\frac{A}{8} \left[\ln 3 + \frac{\pi}{\sqrt{3}} - 2 \right] - \hbar \mathcal{B}. \quad (6.4)$$

Equation (6.3) is valid in the generic case where $\Phi_{\text{as}} \neq 0$. According to (5.42) and (5.44), Φ_{as} is likely to vanish only in a two-component plasma where charges are opposite, $e_- = -e_+$ ($A = 0$), and where both species have the same mass ($\mathcal{B} = 0$). When $\Phi_{\text{as}} \neq 0$, if the charge e_α has a sign opposite to that of Φ_{as} , $\rho_\alpha(x) > \rho_\alpha^B$ at sufficiently large distances x , as shown by (6.3).

6.2 Profile of the total particle density

At the order of calculations, the wall is repulsive for the global particle density everywhere in the Coulomb fluid, as in the classical case [1],

$$\sum_{\alpha} \rho_{\alpha}(x) < \sum_{\alpha} \rho_{\alpha}^B. \quad (6.5)$$

Indeed, according to the structure (1.10) of densities, since $\rho_{\alpha}(x)$ and $1 - \exp[-2x^2/\lambda_{\alpha}^2]$ are positive, the second factor on the r.h.s. of (1.10) is also positive in the considered regime of small parameters. Therefore the effect of the vanishing of wavefunctions near the wall is to lower the density $\rho_{\alpha}(x)$: (1.10) implies that at any distance x from the wall

$$\sum_{\alpha} \rho_{\alpha}(x) < \sum_{\alpha} \rho_{\alpha}^B \left[1 - \frac{1}{2} \kappa_D \beta e_{\alpha}^2 \bar{L}(\kappa_D x) - \beta e_{\alpha} \Phi(x) \right]. \quad (6.6)$$

The contribution from the electrostatic potential drop $\Phi(x)$ to the bound in (6.6) vanishes because of the bulk electroneutrality (1.13), as in the case of $\sum_{\alpha} \rho_{\alpha}^{\text{cl}(\varepsilon)}(x)$. Thus the bound involves only the sum of the contributions from classical screened self-energies. The corresponding geometric repulsion from the wall tends to reduce the density of each species with respect to its bulk value, and we get (6.5).

6.3 Charge density profile

Even if the Coulomb fluid remains globally neutral, when species have different masses, the local charge density $\sum_{\alpha} e_{\alpha} \rho_{\alpha}(x)$ is non zero, as well as the associated electrostatic potential drop $\Phi(x)$. The property holds even in the case of a charge-symmetric two-component plasma where the classical charge density $\sum_{\alpha} e_{\alpha} \rho_{\alpha}^{\text{cl}}(x)$ vanishes for symmetry reasons (because the two species have opposite charges). (The latter cancellation can be checked at first order in ε where, by virtue of (5.47), $\sum_{\alpha} e_{\alpha} \rho_{\alpha}^{\text{cl}(\varepsilon)}$ is proportional to $\sum_{\gamma} e_{\gamma}^3 \rho_{\gamma}^B$.) The charge density profile is organized in various layers with opposite signs which depend on the composition of the fluid.

In the very vicinity of the wall ($x \leq \lambda$), when species have different masses, the charge-density profile exhibits a zeroth-order effect arising from

the cancellations of the various wave-functions over different scales. Indeed, according to (6.1) and (1.13),

$$\sum_{\alpha} e_{\alpha} \rho_{\alpha}(x) \underset{x \leq \lambda \leq \xi_D}{\sim} - \sum_{\alpha} e_{\alpha} \rho_{\alpha}^B e^{-2x^2/\lambda_{\alpha}^2} + e\rho \mathcal{O}(\varepsilon, \kappa\lambda), \quad (6.7)$$

where ρ is the typical particle density. When all masses are equal, $\sum_{\alpha} e_{\alpha} \rho_{\alpha}(x)$ is only of order $e\rho \mathcal{O}(\varepsilon, \kappa\lambda)$ in this region, by virtue of the bulk local charge neutrality.

At distances from the wall large with respect to the quantum lengths, $x \gg \lambda$, the charge density is an effect of order $e\rho \mathcal{O}(\varepsilon, \kappa\lambda)$ which is ruled by the competition between the geometric repulsion from the wall and the electrostatic potential drop (see (6.2)). According to (5.48) and (5.43),

$$\sum_{\alpha} e_{\alpha} \rho_{\alpha}(x) \underset{\lambda \ll x \leq \xi_D}{\sim} \sum_{\alpha} e_{\alpha} \rho_{\alpha}^{\text{cl}(\varepsilon)}(x) + \hbar \mathcal{B} \frac{\kappa_D^2}{4\pi} e^{-\kappa_D x},$$

where, by virtue of (5.47) and (5.40),

$$\sum_{\alpha} e_{\alpha} \rho_{\alpha}^{\text{cl}(\varepsilon)}(x) = -\frac{1}{2} \kappa_D \beta \left(\sum_{\gamma} e_{\gamma}^3 \rho_{\gamma}^B \right) [\bar{L}(\kappa_D x) - \bar{M}(\kappa_D x)]. \quad (6.8)$$

In the case of a charge-symmetric two-component plasma $\sum_{\alpha} e_{\alpha} \rho_{\alpha}(x)$ is purely quantum at distances $x \gg \lambda$.

Eventually, the large-distance behavior of $\sum_{\alpha} e_{\alpha} \rho_{\alpha}(x)$ is merely ruled by the electrostatic potential drop $\Phi(x)$, which includes both quantum and classical effects,

$$\sum_{\alpha} e_{\alpha} \rho_{\alpha}(x) \underset{x \gg \xi_D}{\sim} -\frac{\kappa_D^2}{4\pi} \left[\Phi_{\text{as}}^{\text{cl}(\varepsilon)} - \hbar \mathcal{B} \right] e^{-\kappa_D x}, \quad (6.9)$$

where $\Phi_{\text{as}}^{\text{cl}(\varepsilon)}$ is given in (6.4). As it is the case for the electrostatic potential drop and for particle densities, the charge density includes quantum effects, linear in \hbar , which exist far away from the wall over a few Debye screening lengths.

6.4 Global charge

The wall that we consider does not carry any external surface charge and the global surface electroneutrality (1.15) of the Coulomb fluid is fulfilled, as checked in the present section. At leading order $\mathcal{O}(\varepsilon, \kappa\lambda)$ the global surface charge σ can be decomposed into leading classical and quantum contributions: $\sigma = \sigma^{\text{cl}(\varepsilon)} + \sigma^{\text{qu}(\kappa\lambda)}$, where

$$\sigma^{\text{cl}(\varepsilon)} \equiv \int_0^{+\infty} dx \sum_{\alpha} e_{\alpha} \rho_{\alpha}^{\text{cl}(\varepsilon)}(x), \quad (6.10)$$

and $\sigma^{\text{qu}(\kappa\lambda)}$ is the term of order $\kappa\lambda$ in

$$\int_0^{+\infty} dx \sum_{\alpha} e_{\alpha} \left[\rho_{\alpha}(x) - \rho_{\alpha}^{\text{cl}(\varepsilon)}(x) \right]. \quad (6.11)$$

We recall that, as mentioned after (5.47), the hard-core that must be introduced in order to prevent the classical collapse between opposite charges does not appear at order ε in $\rho_{\alpha}^{\text{cl}}(x)$.

Since the classical densities already obey (1.15), which is enforced by macroscopic electrostatics, $\sigma^{\text{cl}(\varepsilon)}$ and $\sigma^{\text{qu}(\kappa\lambda)}$ must vanish separately. As checked in Ref.[1], the classical contribution $\sigma^{\text{cl}(\varepsilon)}$ of order ε arising from $\sum_{\alpha} e_{\alpha} \rho_{\alpha}^{\text{cl}(\varepsilon)}(x)$ does vanish.

The quantum term $\sigma^{\text{qu}(\kappa\lambda)}$ of order $\kappa\lambda$ arises only from the two quantum terms $-\rho_{\alpha}^B \exp[-2x^2/\lambda_{\alpha}^2]$ and $-\rho_{\alpha}^B \beta e_{\alpha} \Phi^{\text{qu}(\kappa\lambda)}(x)$ in $\rho_{\alpha}(x) - \rho_{\alpha}^{\text{cl}(\varepsilon)}(x)$. Indeed, according to (5.48),

$$\begin{aligned} \rho_{\alpha}(x) - \rho_{\alpha}^{\text{cl}(\varepsilon)}(x) = & -\rho_{\alpha}^B e^{-2x^2/\lambda_{\alpha}^2} - \rho_{\alpha}^B \beta e_{\alpha} \Phi^{\text{qu}(\kappa\lambda)}(x) \\ & - \left\{ \left[\rho_{\alpha}^{\text{cl}(\varepsilon)}(x) - \rho_{\alpha}^B \right] - \rho_{\alpha}^B \beta e_{\alpha} \Phi^{\text{qu}(\kappa\lambda)}(x) \right\} e^{-2x^2/\lambda_{\alpha}^2}. \end{aligned} \quad (6.12)$$

The term in curly brackets is a function of order $\rho_{\alpha}^B \mathcal{O}(\varepsilon, \kappa\lambda)$ which decays exponentially fast over the scale κ^{-1} ; by virtue of (5.23), after multiplication by $\exp[-2x^2/\lambda_{\alpha}^2]$ this term gives a contribution of relative order $\mathcal{O}(\varepsilon \cdot \kappa\lambda, (\kappa\lambda)^2)$ to $\sigma^{\text{qu}(\kappa\lambda)}$ defined in (6.11). Therefore $\sigma^{\text{qu}(\kappa\lambda)} = \sigma_{<}^{\text{qu}(\kappa\lambda)} + \sigma_{>}^{\text{qu}(\kappa\lambda)}$ with

$$\sigma_{<}^{\text{qu}(\kappa\lambda)} \equiv - \int_0^{+\infty} dx \sum_{\alpha} e_{\alpha} \rho_{\alpha}^B e^{-2x^2/\lambda_{\alpha}^2} = -\hbar \frac{1}{2} \sqrt{\frac{\pi\beta}{2}} \sum_{\alpha} \frac{e_{\alpha}}{\sqrt{m_{\alpha}}} \rho_{\alpha}^B \quad (6.13)$$

and

$$\sigma_{>}^{\text{qu}(\kappa\lambda)} \equiv - \int_0^{+\infty} dx \sum_{\alpha} e_{\alpha}^2 \rho_{\alpha}^B \beta \Phi^{\text{qu}(\kappa\lambda)}(x), \quad (6.14)$$

where $\Phi^{\text{qu}(\kappa\lambda)}(x)$ is given in (5.43).

The \hbar -contribution $\sigma_{<}^{\text{qu}(\kappa\lambda)}$ to the global charge σ is canceled by the contribution $\sigma_{>}^{\text{qu}(\kappa\lambda)}$. Therefore, the quantum term $\beta e_{\alpha} \Phi^{\text{qu}(\kappa\lambda)}(x)$ in density profiles, which varies over the classical Debye screening length, can be seen as being enforced by the interplay between the global surfacic electroneutrality condition and the fact that, when wave-functions vanish over different length scales, a charge-density profile appears in the very vicinity of the wall even in the zero-coupling limit (see (2.29)).

The previous calculation can also be interpreted as follows. We notice that $\sigma_{<}^{\text{qu}(\kappa\lambda)}$ and $\sigma_{>}^{\text{qu}(\kappa\lambda)}$ can be viewed as the leading \hbar -terms in the

contributions to σ^{qu} from the regions $x < l$ and $x > l$ respectively, with $\lambda \ll l \ll \xi_D$. Indeed,

$$\sigma_{<}^{\text{qu}(\kappa\lambda)} = \lim_{(\lambda/l) \rightarrow 0} \lim_{(l/\xi_D) \rightarrow 0} \left(\int_0^l dx \sum_{\alpha} e_{\alpha} [\rho_{\alpha}(x) - \rho_{\alpha}^{\text{cl}(\varepsilon)}(x)] \right)^{(\kappa\lambda)}, \quad (6.15)$$

whereas

$$\sigma_{>}^{\text{qu}(\kappa\lambda)} = \lim_{(\lambda/l) \rightarrow 0} \lim_{(l/\xi_D) \rightarrow 0} \left(\int_l^{+\infty} dx \sum_{\alpha} e_{\alpha} [\rho_{\alpha}(x) - \rho_{\alpha}^{\text{cl}(\varepsilon)}(x)] \right)^{(\kappa\lambda)}, \quad (6.16)$$

where $\rho_{\alpha}(x) - \rho_{\alpha}^{\text{cl}(\varepsilon)}(x)$ is given in (6.12). l can be identified with the mean interparticle distance a , by virtue of (1.8). Therefore, since $\lambda \ll a$, $\sigma_{<}^{\text{qu}(\kappa\lambda)}$ can be seen as a surface charge located in the plane $x = 0$, whereas $\sigma_{>}^{\text{qu}(\kappa\lambda)}$ is spread in the fluid over the scale ξ_D . On the other hand, according to (5.39) and (6.13), $\Phi^{\text{qu}(\kappa\lambda)}(x)$ may be written as

$$\Phi^{\text{qu}(\kappa\lambda)}(x) = \int d\mathbf{r}' \sigma_{<}^{\text{qu}(\kappa\lambda)} \delta(x') \phi^{(0)}(\mathbf{r}, \mathbf{r}'). \quad (6.17)$$

The interpretation of the latter equation is that $\Phi^{\text{qu}(\kappa\lambda)}(x)$ is the classically-screened electrostatic potential created by the part of the fluid charge-density profile which is concentrated near the wall.

In the case of an intrinsic semiconductor near a junction, the system of electrons and positive holes in the conduction band can be considered as a two-component Coulomb fluid of charges $-q_e$ and $+q_e$ embedded in a medium of relative dielectric constant ϵ_m . q_e is the absolute value of the electron charge and energy terms involve $e \equiv q_e/\sqrt{\epsilon_m}$ (see the comment after (1.1)). Since the semiconductor is intrinsic, the densities ρ_- and ρ_+ are equal to each other. They are determined from the energy gap E_G and from the effective masses m_-^{eff} and m_+^{eff} by [15]

$$\rho = \rho_{\pm}(\beta) = \frac{1}{4} \left(\frac{2}{\pi\beta\hbar^2} \right)^{3/2} (m_-^{\text{eff}} m_+^{\text{eff}})^{3/4} e^{-\beta E_G/2}. \quad (6.18)$$

Since the system is charge-symmetric, there is no classical contribution to the potential drop $\Phi(x)$ and (1.10) becomes

$$\rho_{\pm}(x) = \rho \left(1 - e^{-2x^2/\lambda_{\pm}^2} \right) \left[1 - \varepsilon \bar{L}(\kappa_D x) \mp \beta \frac{q_e}{\sqrt{\epsilon_m}} \Phi^{\text{qu}}(0) e^{-\kappa_D x} \right], \quad (6.19)$$

where $\varepsilon \equiv \beta q_e^2/(2\epsilon_m)$ and, according to (5.43) and (5.44),

$$\beta \frac{q_e}{\sqrt{\epsilon_m}} \Phi^{\text{qu}}(0) = \frac{1}{4} \sqrt{\frac{\pi}{2}} \kappa_D \lambda_- \left[1 - \sqrt{\frac{m_-^{\text{eff}}}{m_+^{\text{eff}}}} \right]. \quad (6.20)$$

(We notice that on principle the expression (6.19) is valid only when the wall has the same dielectric constant as the medium where charge carriers move.)

In the case of GaSb, $E_G = 0.67 \text{ eV}$ at 273 K , $m_-^{\text{eff}} = 0.047 m_e$, $m_+^{\text{eff}} = 0.5 m_e$ (where m_e is the electron mass), and $\epsilon_m = 15$. This system is in the regime (1.9) for which explicit analytical expressions are calculated in the present paper: $\kappa_D \lambda_- = 2.5 \cdot 10^{-3}$, $\varepsilon = 6 \cdot 10^{-4}$, $(\lambda_-/a)^3 = 2 \cdot 10^{-6}$ (with $(4/3)\pi a^3 \rho_- = 1$). (The length scales are $\lambda_+ \sim 2.5 \text{ nm}$, $\lambda_- \sim 8.3 \text{ nm}$, $a \sim 640 \text{ nm}$ and $\xi_D \sim 3300 \text{ nm}$.) The vanishing of particle densities occurs on two different scales λ_+ and $\lambda_- \sim 3.3\lambda_+$. According to (6.13), where $e_\alpha = \pm q_e$, the resultant surface charge located on the wall (over the width λ_-) is $\sigma_{<}^{\text{qu}(\kappa\lambda)} = 5 \cdot 10^{-14} \text{ C cm}^{-2} = 3 \cdot 10^5 q_e \text{ cm}^{-2}$. The bulk density of charge carriers is $\rho_- + \rho_+ \sim 2 \cdot 10^{12} \text{ cm}^{-3}$ and the charge density at distances $x > a$ is $\rho_c \exp[-\kappa_D x]$ with, according to (6.19) and (6.20), $\rho_c = 10^9 q_e \text{ cm}^{-3}$. Thus $\rho_c \lambda_- \sim 1 q_e \text{ cm}^{-2}$ is indeed negligible compared with $\sigma_{<}^{\text{qu}(\kappa\lambda)}$. The potential drop $\Phi^{\text{qu}}(0) = 1.3 \cdot 10^{-5} \text{ eV}$ remains negligible with respect to the energy gap.

7 Comment

In this section, we comment on the case where the wall is made of a dielectric material, characterized by a relative dielectric constant ϵ_w with respect to the vacuum, when ϵ_w is different from the relative dielectric constant ϵ_m of the medium where charges move. Then the Coulomb interaction reads

$$v_w(\mathbf{r}, \mathbf{r}') = \frac{1}{|\mathbf{r} - \mathbf{r}'|} - \Delta_{\text{el}} \frac{1}{|\mathbf{r} - \mathbf{r}'^*|} \quad (7.1)$$

with $\Delta_{\text{el}} = (\epsilon_w - \epsilon_m)/(\epsilon_w + \epsilon_m)$. The response of the wall induced by the presence of a particle with charge e_α (which includes a factor $1/\sqrt{\epsilon_m}$ in interaction terms) is equivalent to the presence of an image charge at position \mathbf{r}^* , symmetric of the real-particle position \mathbf{r} with respect to the wall, and which carries a charge $-\Delta_{\text{el}} e_\alpha$. The Hamiltonian also involves the self-energy $-\Delta_{\text{el}} e_\alpha^2/4x$, due to the interaction of a particle with its own image charge. The corresponding loop self-energy can be incorporated in the loop fugacity $z(\mathcal{L})$, which now reads

$$z(\mathcal{L}) = z_\alpha \theta(x) \exp \left[\Delta_{\text{el}} \frac{\beta e_\alpha^2}{4} \int_0^1 ds \frac{1}{x + \lambda_\alpha \xi_x(s)} \right]. \quad (7.2)$$

In order to exhibit the screening of the self-energy, which is not integrable at large distances x from the wall, we have performed a resummation in two steps, which generalizes the method devised for classical systems in

Ref.[5]. The choice of the same nine resummed bonds as those in Section 3.2 combined with the two-step resummation leads to resummed weights which are integrable, because they involve only screened loop-fugacities.

Indeed, in the one-step resummation of Section 3.2 the weights corresponding to the nine resummed bonds are $z^{\text{sc}}(\mathcal{L})$ and $z^{\text{sc}}(\mathcal{L}) - z(\mathcal{L})$, instead of the weights $z(\mathcal{L})$ and $z^{\text{sc}}(\mathcal{L}) - z(\mathcal{L})$ that arise when there are only five resummed bonds without any “double” bond, such as $[F^{\text{cc}}]^2/2$, as it is done in Ref.[4]. At the end of the two-step resummation process, the construction rules for resummed diagrams are the same ones as in the one-step resummation of Section 3.2, with the only difference that weights $z^{\text{sc}}(\mathcal{L})$ and $z^{\text{sc}}(\mathcal{L}) - z(\mathcal{L})$ are replaced by weights $z^{\text{sc}[2]}(\mathcal{L})$ and $z^{\text{sc}[2]}(\mathcal{L}) - z^{\text{sc}[1]}(\mathcal{L})$. These weights are integrable at large distances x from the wall, because both $z^{\text{sc}[2]}(\mathcal{L})$ and $z^{\text{sc}[1]}(\mathcal{L})$ result from resummations of Coulomb ring sub-diagrams.

More precisely, the expressions of the resummed loop fugacities $z^{\text{sc}[i]}(\mathcal{L})$ (with $i = 1, 2$) are given by (3.11) and (3.12) where the value of $z(\mathcal{L})$ is that given in (7.2) and $\phi - v$ in $\mathcal{V}_{\text{cloud}}^{\text{sc}}(\mathcal{L})$ is replaced by $\phi_w^{[i]} - v_w$; the $\phi_w^{[i]}$'s have the same boundary conditions as v_w written in (7.1) and they obey the inhomogeneous Debye equation (1.16) where $\overline{\kappa^{[1]}}^2(x) \equiv 4\pi\beta \sum_{\alpha} e_{\alpha}^2 \int \mathcal{D}_{x,\alpha}(\xi) z(\mathcal{L})$ and $\overline{\kappa^{[2]}}^2(x) \equiv 4\pi\beta \sum_{\alpha} e_{\alpha}^2 \int \mathcal{D}_{x,\alpha}(\xi) z^{\text{sc}[1]}(\mathcal{L})$. (Resummed bonds are defined with $\phi_w^{[2]}$ in place of ϕ .)

As a consequence of quantum dynamics, screened loop self-energies (and subsequently particle densities) are found to approach their bulk values only with an integrable $1/x^3$ tail, whereas the particle self-energy due to the electrostatic response of the wall is exponentially screened in classical systems [16, 1]. Even for bulk properties [17, 18], screening in quantum systems is less efficient than in classical fluids.

More precisely, the screened loop self-energy in $z^{\text{sc}[1]}(\mathcal{L})$ or $z^{\text{sc}[2]}(\mathcal{L})$ is the sum of two contributions. The exponentially-decaying part has the same decay at large distances from the wall as the screened self-energy of a classical charge [5]. The algebraic $1/x^3$ tail arises from the other part, which reads

$$\Delta_{\text{el}} \frac{e_{\alpha}^2}{2} \int_0^1 ds \int_0^1 ds' (1 - \delta(s - s')) \frac{1}{|\mathbf{r} + \lambda_{\alpha} \xi(s) - \mathbf{r}^* - \lambda_{\alpha} \xi^*(s')|} \quad (7.3)$$

(See the analogous term (3.9) in the screened pair interaction). In the low-degeneracy and weak-coupling regime the particle density $\rho_{\alpha}(x)$ does not seem to have a simple explicit value, because of the self-energy contributions arising from the dielectric response of the wall.

A : Resummation of large-distance Coulomb divergences

In this appendix, we display the resummation of Coulomb divergences in the Mayer representation (3.2) for the loop-fugacity expansion of the loop density. We use the same decomposition of f -bonds as the one performed in Appendix B of Ref. [4]. (The *a priori* arbitrary decomposition is chosen according to the properties to be studied after resummation.) The f -bond is written as the sum of ten auxiliary bonds \tilde{f} ,

$$f(\mathcal{L}, \mathcal{L}') = \left\{ f^{cc} + f^{mc} + f^{cm} + f^{mm} + \frac{1}{2} [f^{cc}]^2 + f^{cc} f^{mc} + f^{cc} f^{cm} + \frac{1}{2} [f^{mc}]^2 + \frac{1}{2} [f^{cm}]^2 + f_{\text{TT}} \right\} (\mathcal{L}, \mathcal{L}'). \quad (\text{A.1})$$

Bonds f^{cc} , f^{mc} , f^{cm} and f^{mm} are defined from the multipolar decomposition (3.3) and are introduced in order to handle classical exponential screening. These bonds read

$$f^{ab}(\mathcal{L}, \mathcal{L}') = -\beta e_\alpha e_{\alpha'} \mathcal{V}^{ab}(\mathcal{L}, \mathcal{L}'), \quad (\text{A.2})$$

where superscripts a and b stand either for c or m , and where we have set $\mathcal{V}^{cc}(\mathcal{L}, \mathcal{L}') \equiv v(\mathbf{r} - \mathbf{r}')$. f_{TT} is defined by (A.1). Double f -bonds (such as $[f^{cc}]^2/2$, $f^{cc} f^{cm}$, ...) are not involved in the series representation (3.2) where two points can be linked by at most one f -bond. We choose to make them appear in the decomposition (A.1) in order to obtain a finite sum for the contribution from all possible ring subdiagrams which are defined hereafter. When the decomposition (A.1) is introduced in the Mayer representation (3.2) of the loop density, diagrams \mathbb{G} are replaced by diagrams $\tilde{\mathbb{G}}$ built with the ten \tilde{f} -bonds defined in (A.2) and the same topological rules as diagrams \mathbb{G} .

The resummation procedure relies on the integration over the intermediate points (called ‘‘Coulomb points’’) of all possible Coulomb-chain or Coulomb-ring subdiagrams. A Coulomb-chain subdiagram between two points \mathcal{L} and \mathcal{L}' is equal to

$$\int d\mathcal{L}_1 \cdots d\mathcal{L}_N f^{ac}(\mathcal{L}, \mathcal{L}_1) z(\mathcal{L}_1) f^{cc}(\mathcal{L}_1, \mathcal{L}_2) z(\mathcal{L}_2) f^{cc}(\mathcal{L}_2, \mathcal{L}_3) \times \cdots z(\mathcal{L}_N) f^{cb}(\mathcal{L}_N, \mathcal{L}') \quad (\text{A.3})$$

with an arbitrary number $N \geq 1$ of internal points. A Coulomb-ring subdiagram attached to a point \mathcal{L} is a closed Coulomb-chain subdiagram, i.e.

with $\mathcal{L} = \mathcal{L}'$ (see Fig.5). It is equal either to $\int d\mathcal{L}_1 z(\mathcal{L}_1) [f^{cc}(\mathcal{L}, \mathcal{L}_1)]^2 / 2$, $\int d\mathcal{L}_1 z(\mathcal{L}_1) [f^{mc}(\mathcal{L}, \mathcal{L}_1)]^2 / 2$, $\int d\mathcal{L}_1 z(\mathcal{L}_1) f^{cc}(\mathcal{L}, \mathcal{L}_1) f^{mc}(\mathcal{L}, \mathcal{L}_1)$ or

$$\frac{1}{S} \int d\mathcal{L}_1 \cdots d\mathcal{L}_N f^{ac}(\mathcal{L}, \mathcal{L}_1) z(\mathcal{L}_1) f^{cc}(\mathcal{L}_1, \mathcal{L}_2) z(\mathcal{L}_2) f^{cc}(\mathcal{L}_2, \mathcal{L}_3) \times \cdots z(\mathcal{L}_N) f^{cb}(\mathcal{L}_N, \mathcal{L}) \quad (\text{A.4})$$

where S is the symmetry factor of the Coulomb-ring subdiagram ($S = 2$ if $a = b$ and $S = 1$ otherwise). Coulomb-ring subdiagrams do exist in diagrams $\tilde{\mathbb{G}}$, because the latter ones contain articulation points.

Diagrams $\tilde{\mathbb{G}}$ can be collected into classes of a partition where all diagrams $\tilde{\mathbb{G}}$ inside the same class lead to the same prototype diagram \mathbb{P}^* after erasing the intermediate points of all Coulomb-chain or Coulomb-ring subdiagrams. When resummed bonds are defined, some “excluded-composition” rules ensure a one-to-one correspondence between each class in the partition of diagrams $\tilde{\mathbb{G}}$ and each diagram \mathbb{P}^* . In the present paper, we choose to build prototype diagrams \mathbb{P}^* made with bonds F^{cc} , F^{cm} , F^{mc} , $(1/2)[F^{cc}]^2$, $(1/2)[F^{cm}]^2$, $(1/2)[F^{mc}]^2$, $F^{cc}F^{cm}$, $F^{mc}F^{cc}$ and F_{RT} (see (3.7)). This choice leads to resummed diagrams where the new weight of every point is convenient for dealing with the case of a wall with a dielectric response, as explained in Section 7.

The bond $F^{cc}(\mathcal{L}, \mathcal{L}')$ between two loops \mathcal{L} and \mathcal{L}' of a prototype diagram \mathbb{P}^* is defined as the sum of the bond $f^{cc}(\mathcal{L}, \mathcal{L}')$ and of all Coulomb chains involving only f^{cc} -bonds between \mathcal{L} and \mathcal{L}' (see Fig. 2). The bond $F^{mc}(\mathcal{L}, \mathcal{L}')$ is the sum of the bond $f^{mc}(\mathcal{L}, \mathcal{L}')$ and of all Coulomb chains (A.3) with $a = m$ and $b = c$ (see Fig.3). Bonds $[F^{cc}]^2/2$, $[F^{cm}]^2/2$, $[F^{mc}]^2/2$, $F^{cc}F^{cm}$ and $F^{cc}F^{mc}$ between two points \mathcal{L} and \mathcal{L}' originate from subdiagrams with either one bond $(1/2)[f^{cc}]^2$, $(1/2)[f^{cm}]^2$, $(1/2)[f^{mc}]^2$, $f^{cc}f^{cm}$, or $f^{cc}f^{mc}$ respectively, or from subdiagrams with two Coulomb chains between \mathcal{L} and \mathcal{L}' (see Fig.4). In Ref.[4], the prototype diagrams were chosen to be built with only five resummed bonds called F^{cc} , F^{cm} , F^{mc} and F_{R_z} and F_{RT_z} . Since the resummation procedure relies on the integration over the same intermediate points in the same diagrams $\tilde{\mathbb{G}}$ in both cases, the expressions of F^{cc} and F^{mc} are the same (see Eqs. (3.7a) and (3.7b)), while F_{RT} is equal to

$$F_{\text{RT}} = F_{\text{R}_z} - \frac{1}{2}[F^{cc}]^2 - \frac{1}{2}[F^{cm}]^2 - \frac{1}{2}[F^{mc}]^2 - F^{cc}.F^{cm} - F^{cc}.F^{mc}. \quad (\text{A.5})$$

>From the expression of F_{R_z} derived in Ref. [4], we get the value (3.7c).

The “excluded-composition” rule is different from those of Ref.[4], because resummed bonds are different in the present case. The rule arises from the following arguments. When \mathcal{L} is the intermediate point of the

chain $F^{\text{ac}}(\mathcal{L}_i, \mathcal{L}) F^{\text{cb}}(\mathcal{L}, \mathcal{L}_j)$ with $i \neq j$ and is not involved in any other bond, or when \mathcal{L} appears only in one bond $(1/2) [F^{\text{ac}}(\mathcal{L}_i, \mathcal{L})]^2$ (with $a = c$ or m) or one bond $F^{\text{cc}}(\mathcal{L}_i, \mathcal{L}) F^{\text{mc}}(\mathcal{L}_i, \mathcal{L})$, the reason why \mathcal{L} has not disappeared in the resummation process can only be that \mathcal{L} carried at least one Coulomb ring in every diagram $\tilde{\mathbb{G}}$ in the class which leads to the diagram \mathbb{P}^* after erasing Coulomb points. Therefore, after integration over Coulomb points, the weight $z(\mathcal{L})$ attached to point \mathcal{L} in diagrams $\tilde{\mathbb{G}}$ is multiplied in diagrams \mathbb{P}^* by the sum of all products of Coulomb rings attached to \mathcal{L} . As argued in Ref.[4], the sum is equal to $\exp I_r - 1$, where I_r is the sum of all possible Coulomb rings (see Fig. 5). The corresponding weight is equal to $z^{\text{sc}}(\mathcal{L}) - z(\mathcal{L})$ where $z^{\text{sc}}(\mathcal{L}) \equiv z(\mathcal{L}) \exp I_r$. I_r is linked to the screened potential ϕ by $I_r = -\beta e_\alpha^2 \mathcal{V}_{\text{cloud}}^{\text{sc}}$ where $\mathcal{V}_{\text{cloud}}^{\text{sc}}$ is defined in (3.12). $z^{\text{sc}}(\mathcal{L})$ exhibits the stabilizing effect of screening clouds [5]. When \mathcal{L} is not involved only in a product $F^{\text{ac}}(\mathcal{L}_i, \mathcal{L}) F^{\text{cb}}(\mathcal{L}, \mathcal{L}_j)$ (where \mathcal{L}_i may coincides with \mathcal{L}_j), \mathcal{L} may carry no Coulomb ring in the diagrams $\tilde{\mathbb{G}}$ of the corresponding class, and its weight in diagrams \mathbb{P}^* is equal to $z^{\text{sc}}(\mathcal{L})$.

B : Scaling analysis

In this appendix, we perform the scaling analysis of diagrams with one internal point in the resummed Mayer expansion (3.10).

B.1 F^{mc} - and F^{cm} -bonds

A simple scaling analysis of the contribution from diagrams with either one bond $F^{\text{cm}}(\mathcal{L}, \mathcal{L}')$ or one bond $F^{\text{mc}}(\mathcal{L}, \mathcal{L}')$ is obtained by a Taylor expansion of their expressions (see (3.7b)) around their classical values.

In the case of diagram with one bond F^{mc} the Taylor expansion in the variable $\lambda_\alpha \boldsymbol{\xi}(s)$ can be factorized: the leading order is given by

$$\int_0^1 ds \lambda_\alpha \boldsymbol{\xi}(s) \cdot \nabla_{\mathbf{r}} \left(\int d\mathcal{L}' F^{\text{cc}}(\mathcal{L}, \mathcal{L}') z^{\text{sc}}(\mathcal{L}') \right). \quad (\text{B.1})$$

According to the discussion in Section 5.4, at leading order the parenthesis proves to be a function of \mathbf{r} which varies over the scale κ^{-1} . By using the fact that the action of the gradient $\lambda_\alpha \nabla_{\mathbf{r}}$ on a function of $\kappa \mathbf{r}$ multiplies its order by $\kappa \lambda_\alpha$, we get from (5.22) that

$$\int d\mathcal{L}' F^{\text{mc}}(\mathcal{L}, \mathcal{L}') z^{\text{sc}}(\mathcal{L}') = \mathcal{O}(\varepsilon \cdot \kappa \lambda, (\kappa \lambda)^2). \quad (\text{B.2})$$

The diagram with one bond $F^{\text{cm}}(\mathcal{L}, \mathcal{L}')$ involves integrated moments of $\boldsymbol{\xi}'$, which depend on λ_γ , and $\sum_\gamma e_\gamma z_\gamma$ can no longer be factorized at

leading order. Moreover, the first moment of the x -component of ξ does not vanish, and the order of $\int d\mathcal{L}' F^{\text{cm}}(\mathcal{L}, \mathcal{L}') z^{\text{sc}}(\mathcal{L}')$ is given by

$$\sum_{\gamma} z_{\gamma} \int d\mathbf{r}' \left(\int_0^1 ds \int \mathcal{D}_{x', \gamma}(\xi') \xi'_{x'}(s) \right) \lambda_{\gamma} \frac{\partial F^{\text{cc}}(\mathbf{r}, \mathbf{r}')}{\partial x'} \quad (\text{B.3})$$

At leading order $\lambda_{\gamma} \partial F^{\text{cc}}(\mathbf{r}, \mathbf{r}') / \partial x'$ is a function of $\kappa \mathbf{r}$ and $\kappa \mathbf{r}'$, while, as can be checked in (2.18), the mean extension of a Brownian path, $\int_0^1 ds \int \mathcal{D}_{x', \gamma}(\xi') \xi'_{x'}(s)$, vanishes gaussianly fast when x' / λ_{γ} goes to infinity. The latter function makes the next x' -integration convergent over the scale λ (and not κ^{-1}). Therefore, as in (5.23), the order of the integral (B.3) is equal to $\kappa \lambda$ times the order of $z_{\gamma} \int d\mathbf{r}' \lambda_{\gamma} \partial F^{\text{cc}}(\mathbf{r}, \mathbf{r}') / \partial x'$. Since at leading order $F^{\text{cc}}(\mathbf{r}, \mathbf{r}')$ is a function of $\kappa \mathbf{r}$ and $\kappa \mathbf{r}'$, the latter integral is of order $\kappa \lambda$ times the order of $z_{\gamma} \int d\mathbf{r}' F^{\text{cc}}(\mathcal{L}, \mathcal{L}')$, which is equal to $\mathcal{O}(1)$ by virtue of (5.21). Eventually

$$\int d\mathcal{L}' F^{\text{cm}}(\mathcal{L}, \mathcal{L}') z^{\text{sc}}(\mathcal{L}') = \mathcal{O}\left((\kappa \lambda)^2\right). \quad (\text{B.4})$$

B.2 Multiple bonds

In the case of multiple bonds, the dependence upon the species of the loop \mathcal{L}' is not reduced to $e_{\gamma} z_{\gamma}$. Therefore, contrary to what happens in the case of F^{cc} , the neutrality constraint on fugacities (2.11) no longer increases the actual order with respect to that given by pure scaling analysis. For instance, since $[F^{\text{cc}}]^2$ is proportional to $\varepsilon^2 \left[\tilde{\phi}^{(0)}(\tilde{\mathbf{r}}, \tilde{\mathbf{r}}') \right]^2$, while F^{cc} is proportional to $\varepsilon \tilde{\phi}^{(0)}(\tilde{\mathbf{r}}, \tilde{\mathbf{r}}')$, (5.21) implies that

$$\int d\mathcal{L}' \frac{1}{2} [F^{\text{cc}}]^2(\mathcal{L}, \mathcal{L}') z^{\text{sc}}(\mathcal{L}') = \mathcal{O}(\varepsilon). \quad (\text{B.5})$$

However, owing to the construction rule (3.13) about fugacities, the internal point in the diagram made with one bond $[F^{\text{cc}}]^2 / 2$ has a weight equal to $[z^{\text{sc}}(\mathcal{L}') - z(\mathcal{L}')]$. By virtue of (5.15), the latter weight is of order $\mathcal{O}(z\varepsilon)$ and (B.5) leads to

$$\int d\mathcal{L}' \frac{1}{2} [F^{\text{cc}}]^2(\mathcal{L}, \mathcal{L}') [z^{\text{sc}}(\mathcal{L}') - z(\mathcal{L}')] = \mathcal{O}(\varepsilon^2). \quad (\text{B.6})$$

Similarly diagrams $[F^{\text{cc}} F^{\text{mc}}](\mathcal{L}, \mathcal{L}')$ and $\frac{1}{2} [F^{\text{mc}}]^2(\mathcal{L}, \mathcal{L}')$ also have an internal point which carries the weight $z^{\text{sc}}(\mathcal{L}') - z(\mathcal{L}')$. Only the moments of the Brownian path ξ , which is associated with the nonintegrated position

x , are involved and, according to the argument leading to (B.2) and by virtue of (B.6), the contributions from these diagrams are

$$\int d\mathcal{L}' [F^{c\ c} F^{m\ c}] (\mathcal{L}, \mathcal{L}') [z^{sc}(\mathcal{L}') - z(\mathcal{L}')] = \mathcal{O}(\varepsilon^2 \cdot \kappa\lambda) \quad (\text{B.7})$$

and

$$\int d\mathcal{L}' \frac{1}{2} [F^{m\ c}]^2 (\mathcal{L}, \mathcal{L}') [z^{sc}(\mathcal{L}') - z(\mathcal{L}')] = \mathcal{O}(\varepsilon^2 \cdot (\kappa\lambda)^2). \quad (\text{B.8})$$

For the bond $[F^{c\ c} F^{c\ m}]$, by virtue of the mechanism involved in (B.4), the integration over x' of the first moment of the Brownian path ξ' leads to an extra factor $(\kappa\lambda)^2$ with respect to the order (B.5) of the contribution from $[F^{c\ c}]^2/2$, namely

$$\int d\mathcal{L}' [F^{c\ c} F^{c\ m}] (\mathcal{L}, \mathcal{L}') z^{sc}(\mathcal{L}') = \mathcal{O}(\varepsilon \cdot (\kappa\lambda)^2). \quad (\text{B.9})$$

At leading order the bond $[F^{c\ m}]^2/2$ involves the second moment of the Brownian path ξ' . This moment tends to a non-zero value when x goes to infinity, so that the integration over x' still converges over the scale κ^{-1} . Therefore, according to the argument leading to (B.2), the order of the contribution from $[F^{c\ m}]^2/2$ has an extra factor of order $(\kappa\lambda)^2$ with respect to (B.5),

$$\int d\mathcal{L}' \frac{1}{2} [F^{c\ m}]^2 (\mathcal{L}, \mathcal{L}') z^{sc}(\mathcal{L}') = \mathcal{O}(\varepsilon \cdot (\kappa\lambda)^2). \quad (\text{B.10})$$

B.3 F_{RT} -bond

Let us consider the diagram made of a single bond F_{RT} . The integration over the Brownian path ξ' makes the integral over \mathbf{r}' convergent at small distances $|\mathbf{r} - \mathbf{r}'|$. The order of the contribution from this diagram can be inferred from the known results about the bond F_{RT}^* obtained by adding to F_{RT} the double bonds different from $[F^{c\ c}]^2/2$, which do not contribute to the integrability of F_{RT} at large distances $|\mathbf{r} - \mathbf{r}'|$ in the limit where ε vanishes. F_{RT}^* is defined by

$$F_{\text{RT}} = F_{\text{RT}}^* - \frac{1}{2} [F^{c\ m}]^2 - \frac{1}{2} [F^{m\ c}]^2 - F^{c\ c} \cdot F^{c\ m} - F^{c\ c} \cdot F^{m\ c}. \quad (\text{B.11})$$

where F_{RT} is given in (3.7c).

The order of the contribution of $\int d\mathbf{r}' \int \mathcal{D}_{x,\alpha}(\xi) \int \mathcal{D}_{x',\gamma}(\xi') F_{\text{RT}}^*(\mathcal{L}, \mathcal{L}')$ has been studied in the bulk situation in Ref.[19] (and a similar calculation also appears in Ref.[20]). Let us introduce the thermal de Broglie wavelength $\lambda_{\alpha\gamma}$ associated with the reduced mass $m_\alpha m_\gamma / (m_\alpha + m_\gamma)$. In the

bulk, the considered integral proves to be the sum of a term of order $\lambda_{\alpha\gamma}^3$ times an analytic function $Q(\xi_{\alpha\gamma})$ of the parameter $\xi_{\alpha\gamma} \equiv -\beta e_\alpha e_\gamma / \lambda_{\alpha\gamma}$ [14], plus a term of order $(\beta e_\alpha e_\gamma) \lambda^2$ (with two contributions where $\lambda = \lambda_\alpha$ or $\lambda = \lambda_\gamma$). The latter “diffraction” term arises from the second moments of the Brownian paths. There is no term proportional to $(\beta e_\alpha e_\gamma)^2 \lambda$, because the first moment of a Brownian path vanishes in the bulk, by virtue of the spherical symmetry.

In the vicinity of the wall, the precise calculation is more delicate than in the bulk. However, we may expect to obtain the same orders $\lambda_{\alpha\gamma}^3$ and $(\beta e_\alpha e_\gamma) \lambda^2$ as in the bulk, plus a term of order $(\beta e_\alpha e_\gamma)^2 \lambda$ allowed by the anisotropy introduced by the presence of the wall. Since the fugacity $z^{\text{sc}}(\mathcal{L}')$ is of order $\mathcal{O}(\rho) = \mathcal{O}(a^{-3})$, the contribution from the diagram made of a single F_{RT} -bond can be viewed as the sum of four terms with respective orders

$$\left(\frac{\lambda}{a}\right)^3 Q_w \left(-\frac{\beta e_\alpha e_\gamma}{\lambda_{\alpha\gamma}}\right), \quad (\text{B.12})$$

where Q_w is defined similarly to Q mentioned previously [14] with the only difference that space integrals are restricted to $x > 0$ and $x' > 0$,

$$\left(\frac{\beta e_\alpha e_\gamma}{a}\right) \left(\frac{\lambda}{a}\right)^2 = \mathcal{O}((\kappa\lambda)^2), \quad (\text{B.13})$$

$$\left(\frac{\beta e_\alpha e_\gamma}{a}\right)^2 \left(\frac{\lambda}{a}\right) = \mathcal{O}(\varepsilon \cdot \kappa\lambda), \quad (\text{B.14})$$

and

$$\left(\frac{\beta e_\alpha e_\gamma}{a}\right)^3 \ln(\kappa\lambda) = \mathcal{O}(\varepsilon^2 \ln(\kappa\lambda)). \quad (\text{B.15})$$

In these equalities we have used the relations (1.6) and (5.1).

References

- [1] J.-N. Aqua and F. Cornu. Density profile in a classical Coulomb fluid near a dielectric wall. I. *J. Stat. Phys.*, **105**:211, 2001.
- [2] B. Jancovici. Sum rules for inhomogeneous Coulomb fluids, and ideal conductor boundary conditions. *J. Physique*, **47**:389–392, 1986.
- [3] A. Alastuey, F. Cornu, and A. Perez. Virial expansions for quantum plasmas: Diagrammatic resummations. *Phys. Rev. E*, **49**:1077, 1994.
- [4] F. Cornu. Correlations in quantum plasmas. I. Resummations in Mayer-like diagrammatics. *Phys. Rev. E*, **53**:4562, 1996.

- [5] J.-N. Aqua and F. Cornu. Density profile in a classical Coulomb fluid near a dielectric wall. II. *J. Stat. Phys.*, **105**:245, 2001.
- [6] E. Lieb and J.L. Lebowitz. The constitution of matter : Existence of thermodynamics for systems composed of electrons and nuclei. *Adv. Math.*, **9**:316, 1972.
- [7] F. Cornu. In preparation.
- [8] M. Kac. *Probability and Related Topics in Physical Science*. Wiley Interscience, New York, 1959.
- [9] B. Simon. *Functionnal Integration and Quantum Physics*. Academic, New York, 1969.
- [10] J.-N. Aqua and F. Cornu. Classical and quantum algebraic screening in a Coulomb plasma near a wall : a solvable model. *J. Stat. Phys.*, **97**, 1999.
- [11] E. Meeron. Theory of potentials of average force and radial distribution functions in ionic solutions. *J. Chem. Phys.*, **28**:630, 1958.
- [12] J.-N. Aqua and F. Cornu. Dipolar effective interaction in a fluid of charged spheres near a dielectric plate. *Phys. Rev. E*, **68**:026133, 2003.
- [13] D. Zwillinger. *Handbook of differential equations*. Academic Press, 1989.
- [14] W. Ebeling. Coulomb interaction and ionization equilibrium in partially ionized plasmas. *Physica*, **43**:293, 1969.
- [15] Ashcroft N.W. and N.D. Mermin. *Solid State Physics*. Holt-Saunders International, 1976.
- [16] L. Onsager and N.T. Samaras. The surface tension of Debye-Hückel electrolytes. *J. Chem. Phys.*, **2**:528–536, 1934.
- [17] A. Alastuey and Ph. A. Martin. Absence of exponential clustering in quantum Coulomb fluids. *Phys. Rev. A*, **40**:6485, 1989.
- [18] F. Cornu. Correlations in quantum plasma. II. Algebraic tails. *Phys. Rev. E*, **53**:4595, 1996.
- [19] F. Cornu. Quantum plasmas with or without a uniform field. II. Exact low-density free energy. *Phys. Rev. E*, **58**:5293, 1998.
- [20] A. Alastuey, F. Cornu, and A. Perez. Virial expansions for quantum plasmas: Maxwell-Boltzmann statistics. *Phys. Rev. E*, **51**:1725, 1995.